CEAS Aeronautical Journal
https://doi.org/10.1007/s13272-024-00759-1

ORIGINAL PAPER

Battery-electric powertrain system design for the HorizonUAM multirotor air taxi concept

Florian Jäger[1] · Oliver Bertram[1] · Sascha M. Lübbe[1] · Alexander H. Bismark[1] · Jan Rosenberg[1] · Lukas Bartscht[1]

Received: 20 October 2023 / Revised: 29 May 2024 / Accepted: 1 July 2024

Abstract

The work presented herein has been conducted within the DLR internal research project HorizonUAM, which encompasses research within numerous areas related to urban air mobility. One of the project goals was to develop a safe and certifiable onboard system concept. This paper aims to present the conceptual propulsion system architecture design for an all-electric battery-powered multirotor electric Vertical Takeoff and Landing (eVTOL) vehicle. Therefore, a conceptual design method was developed that provides a structured approach for designing the safe multirotor propulsion architecture. Based on the concept of operation the powertrain system was initially predefined, iteratively refined based on the safety assessment and validated through component sizing and simulations. The analysis was conducted within three system groups that were developed in parallel: the drivetrain, the energy supply and the thermal management system. The design process indicated that a pure quadcopter propulsion system can merely be designed reasonably for meeting the European Union Aviation Safety Agency (EASA) reliability specifications. By adding two push propellers and implementing numerous safety as well as passivation measures the reliability specifications defined by EASA could finally be fulfilled. The subsequent system simulations also verified that the system architecture is capable of meeting the requirements of the vehicle concept of operations. However, further work is required to extend the safety analysis to additional system components as the thermal management system or the battery management system and to reduce propulsion system weight.

Keywords Urban air mobility · Conceptual aircraft design · Model-based safety assessment · Propulsion system · Multirotor · eVTOL

Abbreviations

ARP	Aerospace Recommended Practice
EASA	European Union Aviation Safety Agency
EASA SC E-19	Special Condition for Electric / Hybrid Propulsion System
EASA SC-VTOL	Special Condition for Vertical Takeoff and Landing Vehicle defined by the EASA
eVTOL	Electric Vertical Takeoff and Landing
FCC	Flight Control Computer
FDAL	Function Development Assurance Level
FHA	Functional Hazard Analysis
FIT	Failure in Time
FTA	Fault Tree Analysis
MTBF	Mean Time Between Failures
MTOM	Maximum Takeoff Mass
MTTF	Mean Time to Failure
NPRD	Nonelectronic Parts Reliability Data
PASA	Preliminary Aircraft Safety Assessment
PMSM	Permanent Magnet Synchronous Motor
PSSA	Preliminary System Safety Assessment
UAM	Urban Air Mobility
UAS	Unmanned Aerial System
VTOL	Vertical Takeoff and Landing

✉ Florian Jäger
florian.jaeger@dlr.de

[1] DLR Institute of Flight Systems, German Aerospace Center, Lilienthalplatz 7, Braunschweig 38108, Germany

Published online: 31 July 2024

1 Introduction

As the majority—over 54 % (4.5 billion people)—of the world population is already living in urban areas and this trend is projected to continue up to 68 % (6.68 billion people) by 2050, new, efficient and zero-emission transportation methods will play a major role in organizing the future mobility needs [1]. Already today, people within the biggest cities experience traffic delays of more than 100 h per person within a year [2]. Since the ongoing urbanization will most probably lead to further congestion while the road infrastructure cannot be increased unlimited, new alternatives to existing travel methods need to be established. The vision of Vertical Takeoff and Landing (VTOL) vehicle operation (ops) is to relocate some of the travel from the road up into the air and, thereby, contribute in reducing traffic jams, improving the mobility and reducing the personal travel time [3, 4] for a portion of today's travel demand. Another major challenge in the ongoing trend of urbanization is that today 45 % of all CO2 emissions from global transportation is produced by the road traffic [5]. Using electrified propulsion systems for VTOL vehicle may contribute in providing low-emission transportation means especially when using renewable energy sources [3, 6]. Lastly and more importantly, concepts for electrified VTOL vehicle can pave the way towards electric powered aircraft as they may be one of the first suitable use cases so far. 30.6 % of all flights within Europe cover a flight distance of less than 500 km [7]. Those flights may offer the chance to be conducted by electric aircraft [8, 9].

Due to these challenges in transportation and the potentials for VTOL vehicles, several hundred vehicle concepts have been unveiled and are worked on by aircraft manufacturers, start-ups, automotive manufacturers as well as research facilities [10]. The first certified operation with passengers on board is expected to take place already in the mid-2020 s [11]. One of the main challenges preventing VTOL vehicle with passengers on board being operated today is the unproven safety and reliability of those concepts as well as missing certification standards. Beginning in 2018, the European Union Aviation Safety Agency (EASA) started the process of developing and defining a certification basis, named the Special Condition for VTOL vehicle (EASA SC-VTOL), as well as the corresponding means of compliance [12] for such vehicles. The safety objectives stated therein for the category enhanced aircraft[1] set high standards similar to commercial aviation. For example, the vehicle must be able for a continued safe flight and landing even if any single system failure or a combination of failures that are not classified as catastrophic occur. Additionally, a catastrophic failure condition must have a failure rate of less than 10^{-9} failures per flight hour and must not result from a single failure. As a reliable propulsion system is crucial for a safe VTOL operation, the design of the vehicle's propulsion system takes over an important role. So far, there has only been little research focus on analyzing the propulsion system reliability and its effects on the safe vehicle operation. However, the research that has already been conducted, indicates that the EASA safety objectives are especially difficult to meet for wingless multirotor concept vehicles [13–15]. This work, therefore, addresses these challenges and aims to present the conceptual design process of developing a safe propulsion system for multirotor electric Vertical Takeoff and Landing (eVTOL) vehicles as well as its implications when being applied to an exemplary use case. The goal is to provide further insights into the conceptual design to facilitate the development of the propulsion system architecture and its certification for similar eVTOL vehicle. The research presented herein has been conducted by the Safety-Critical Systems and Systems Engineering department of the DLR Institute of Flight Systems within the DLR internal project HorizonUAM.

1.1 Research questions and methodological approach

In contribution to the aim of this work, the following research questions will be covered:

1. How should the conceptual design process of the propulsion system be carried out for an all-electric multirotor VTOL vehicle that is transporting passengers over congested areas so that the safety goals of EASA SC-VTOL can be met?
2. What is the impact of the EASA SC-VTOL reliability requirements on the conceptual design of a multirotor propulsion system?
3. Which specific design and sizing characteristics must be considered for an battery-electric propulsion system architecture apart from the safety requirements?
4. Which requirements must be met by a thermal management system of the developed all-electric multirotor propulsion system?

To address these research questions, chapter 2 describes the methodological approach for the conceptual design of a safe propulsion system for a quadcopter eVTOL vehicle. In chapter 3, the methodological approach is applied using an exemplary eVTOL use case of the HorizonUAM project. Up to Sect. 3.2, an initial propulsion system concept is developed, which is further detailed and refined within Sect. 3.3 based on the safety design process. For the derived propulsion system architecture, the power and drive system, the thermal

[1] Vehicles that are transporting passengers over congested areas fall into the category enhanced of the EASA SC-VTOL [12].

management system (TMS) and the electrical system, are then sized and simulated and final architecture adjustments deducted within Sects. 3.4.1, 3.4.2 and 3.4.3. The Sect. 3.5 presents the final propulsion architecture. Within chapter 4 the main findings are summarized and the initial research questions answered. The paper is completed by deriving current limitations of the applied methodology and giving an outlook for further research within chapter 5.

1.2 State of the art

At first, a literature research was conducted to identify the current state of the art regarding conceptual design methodologies for developing the propulsion system for multirotor vehicles, that also take safety requirements into account. Only little literature could be found that addresses this research area so far.

Conceptual design methods for the multirotor propulsion systems

In 2021, Bertram et al. [16] developed a sizing loop which supports the initial multirotor vehicle sizing process based on flight mission requirements and the propulsion technology to be used. However, this method does not provide any detailed information about the propulsion system architecture design and its reliability or failure probabilities. In the work of Liscouët et al. [15] from 2022, a method for the conceptual design of multirotors is presented which includes a controllability analysis, a sizing optimization as well as a safety assessment. However, the controllability analysis does not take flight phase transitions and handling quality aspects into account and so far, the applicability of the safety assessment was only shown based on the Unmanned Aerial System (UAS) regulations. The applicability of this approach for manned eVTOL vehicles therefore is still due.

Currently achieved failure rates of multirotor eVTOL vehicle architectures

In 2019, Darmstadt et al. [13] conducted several safety analyses for the propulsion systems of in total four VTOL configurations, including a tilt-wing, quadcopter, lateral-twin and lift & cruise configuration. For all developed propulsion system architectures, a failure rate in the magnitude of 10^{-4} per flight hour was identified, with the quadcopter configuration having the highest failure rate of $7.97 \cdot 10^{-4}$ per hour. The major challenges for multirotors in meeting the EASA SC-VTOL are that "a single failure must not have a catastrophic effect upon the aircraft" (VTOL.2550) and that a catastrophic event must not happen more often than once every 10^9 flight hours [12]. The work of Liscouët et al. [15] also came to the conclusion that their unmanned quadcopter failure rate lies in the magnitude of $1.44 \cdot 10^{-4}$ per hour and can effectively be reduced by adding more rotors. Using at least eight rotors—which implies a coaxial quadcopter or octocopter configuration—the EASA SC-VTOL could be fulfilled according to their studies.

In 2021, Darmstadt et al. [14] renewed the propulsion architectures from 2019 focusing on the challenging multirotor configurations to improve their reliability and additionally expanded their safety assessment. The failure probability for the quadcopter configuration experiencing catastrophic events could be improved to $1.78 \cdot 10^{-9}$ per hour when using cross-shafts that connect all four main rotor drives. Without using a cross-shaft solution the highest failure probability increases up to $1.75 \cdot 10^{-5}$ per hour. Only by adding numerous redundancies, the failure probability could be reduced to $1.06 \cdot 10^{-9}$ per hour which may be a suitable solution. Therein, the thermal management system was identified as a critical supplementary system, which needed to be dual redundant. However, the consequences of adding these redundancies on vehicle mass, complexity and feasibility of the design have not been further analysed. The difficulty of meeting the EASA SC-VTOL reliability goals shows that a new approach is needed that integrates the safety and reliability assessment into the conceptual design. Additionally, the implications of a safe multirotor propulsion architecture on the vehicle design, mass, the feasibility and complexity need to be readily analysed within the approach to show whether or not the system architecture should be pursued.

The rules and regulations that must be considered within the design process are the already mentioned EASA SC-VTOL, the SC E-19 that define the special condition for electric or hybrid propulsion systems intended for VTOL aircraft as well as the Aerospace Recommended Practice (ARP) 4754A and ARP4761 that define certification considerations and safety assessment guidelines [12, 17–19].[2]

Therefore, this work will present a methodological approach which was applied for the conceptual design of an all-electric propulsion system for a quadcopter that aims at fulfilling EASA SC-VTOL, takes into consideration ARP4761 as well as the Special Condition for Electric / Hybrid Propulsion System (EASA SC E-19) [19] and further analyses its consequences on critical vehicle and flight mission parameters.

2 Method

The applied methodological approach for designing a propulsion system consists of the following steps as indicated in Fig. 1:

[2] For completeness, it is noted that the CS-P defines the certification specifications for the propellers and should also be taken into consideration during the propulsion architecture design [20]. However, they are out of scope of this work.

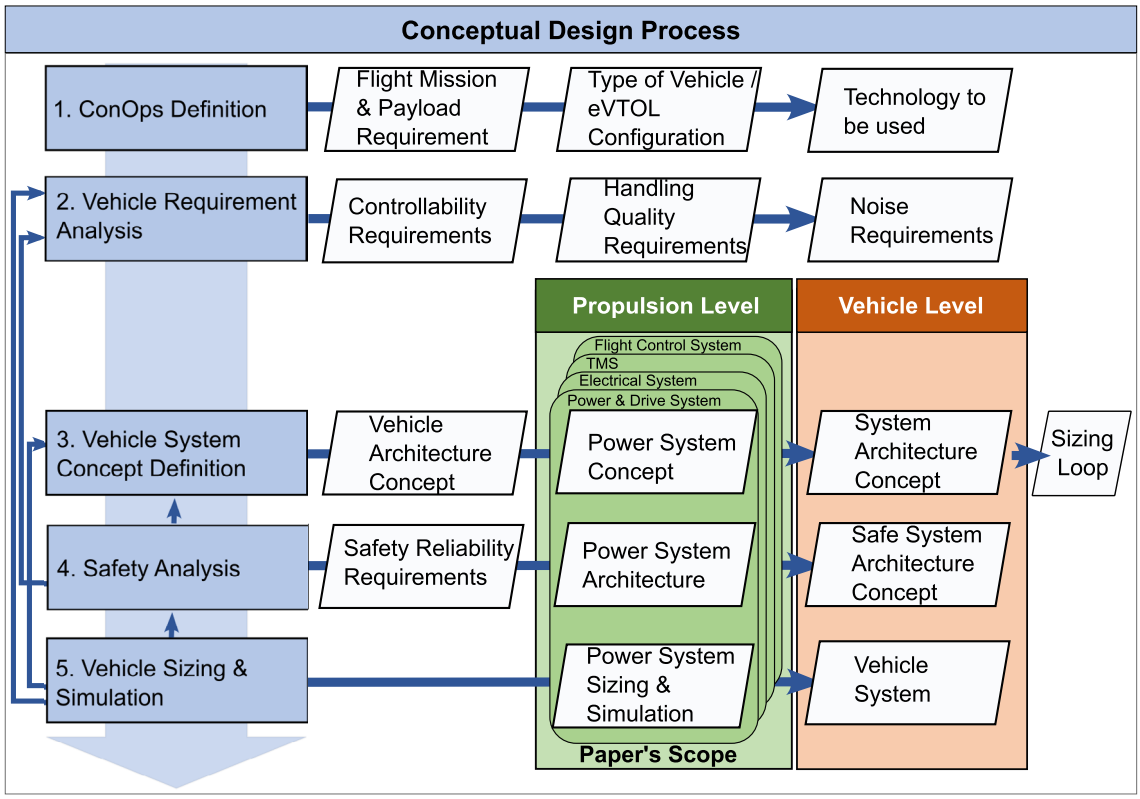

Fig. 1 Applied methodological approach for the conceptual propulsion system design

1. ConOps Definition
2. Vehicle Requirement Analysis
3. Vehicle System Concept Definition
4. Safety Analysis
5. Vehicle Sizing & Simulation

In the first step, the concept of operations (ConOps), the flight mission as well as the payload requirements are defined. Based on this information the best suitable type of vehicle is preselected. Thereafter, the propulsion technology for the selected vehicle is defined.

In the second step, further design requirements for the propulsion system and its components are derived. Several topics should be included herein, among them controllability, handling quality and noise aspects, as they may heavily influence the propulsion system design. It is important to note, that these requirements need to be defined in such a way, that they can be considered within the subsequent sizing loop of step three. Therefore, mathematical models are used, which describe the correlation between the corresponding requirement and the sizing loop design parameters (e.g. power, size, weight).

The ConOps definition and the requirement analysis are the basis for step three, the vehicle system concept definition which includes the propulsion system design loop. Within this step, an initial system concept consisting of the propulsion system as well as the other vehicle systems is defined. Thereby, the propulsion system is specified in terms of the power and drive system, electrical system, the thermal management system and the flight control system. Based on the initial vehicle system architecture concept a first vehicle sizing loop is performed to derive vehicle parameters as, for example, the required vehicle propulsion power, the required energy, vehicle empty weight and rotor size.

In the fourth step, a safety and reliability analysis is conducted for the initial vehicle system architecture, in order to fulfil the EASA SC-VTOL safety goals. Any architecture changes are then passed back to the vehicle system concept.

Within the last step, the safe vehicle architecture is modelled and simulated to validate the suitability of the derived vehicle architecture based on the ConOps definition and vehicle requirement analysis.

As this paper focuses on the propulsion system architecture concept, emphasis is put on presenting steps three, four and five primarily for the propulsion system. The steps one and two are only briefly described in order to provide the context for the propulsion system design.

2.1 ConOps definition

When detailing the ConOps, the type of eVTOL vehicle needs to be selected based on the intended use case and payload requirements. As shown by Ratei [21], different vehicle concepts may be suitable for different operating areas. For example, a rotary-wing concept like a multirotor, or fixed-wing concepts like the lift & cruise, or vectored thrust configurations with tilted wing, tilted rotors or tilted ducts may be suitable.

As soon as the flight mission is defined and the eVTOL vehicle is chosen, the propulsion technology to be used should be evaluated. Propulsion systems like a full-electric battery-powered or hydrogen powered system or even serial or parallel hybrid electric solutions may be suitable.[3]

2.2 Vehicle requirement analysis

Within step two, several further design requirements, primarily for the propulsion system design are collected. As the flight control functions are primarily taken over by the propulsion system within eVTOL vehicles, controllability and handling quality requirements have a significant impact on the propulsion system design and should therefore already be considered at an early design stage. The controllability analysis aims at ensuring, that the vehicle is controllable around all axes. This requires that the Newton's law for translation and rotation need to be fulfilled. As described within Liscouët et al. [15], it is essentially not only to analyse the controllability during normal operating conditions, but also for any failure cases. The difficulty during this step is that the failure cases are not known in the beginning. Therefore, the controllability for failure cases needs to be analysed again when having identified the failure cases within step four, the safety analysis. In general, the controllability depends on whether rotor speed control or pitch control is used and is influenced by the vehicle moment of inertia, the number of rotors, the rotor arrangement, additional rotor parameters (e.g. rotor inertia) and the thrust coefficient of the corresponding rotors [23]. In addition to the controllability aspects, the handling qualities should be considered. According to Pavel [23], the handling qualities of a multirotor are influenced not only by the aircraft response to a control input (controllability) but also to the coupled rotor–motor dynamics. The dynamic response of a coupled rotor–motor drive system, is beneficially influenced by a low rotor inertia, low inertia of the drive components (motor and gearbox), a drive system gear ratio which is optimized for high motor efficiency, balanced motor performance,[4] a low motor equivalent resistance and low friction losses within the drive system which are influenced by the rotational speed and the gear ratio [23]. All influencing parameters combined result in good handling qualities when the dynamic response around all axes is characterised by low rise time, high bandwidth, low overshoot and high stability in terms of phase and gain margin [23]. According to the analysis of Bahr et al. [24] and Niemiec et al. [25] for rotor speed-controlled quadcopters, the weight of the electric motors that are only sized based on the maximum required power demand for performing the flight mission, is insufficient for meeting handling quality requirements. As a high motor torque capability is required for achieving a low motor time constant and therefore good handling qualities, the motor becomes twice as heavy as initially sized. The sum of all electric motors might reach $15-16$ % of the total vehicle weight in case a direct drive is used. Therefore, the factors influencing the handling qualities should already be considered within the conceptual design phase to minimize the design adjustments at a later design phase.[5]

When designing the propulsion architecture, the noise level as well as the effect of noise annoyance should be taken into account in order ensure public acceptance [29]. The eVTOL architecture parameters type of rotor control, maximum rotor tip speed, number of rotors, rotor arrangement, disc loading and the propulsion system architecture should be carefully chosen, as they mainly influence the emitted noise according to Brown and Harris [30], Smith et al. [31] and Smith et al. [32].

An overview of the different parameters and their optimum values is given within Fig. 2.

2.3 Propulsion system concept definition

Taking all the aspects of the ConOps definition and the vehicle requirements analysis into consideration, a first propulsion concept is established. In this step, all systems are identified that are required within the eVTOL propulsion system. At this point, it is important to differentiate between the different nomenclature that is used to describe the propulsion systems. Herein the nomenclature offered by Hermann and Rothfuss [33] is followed in which the propulsion system encompasses a group of systems that contribute to provide lift and power the eVTOL. The propulsion concept was developed by conducting the following steps:

[3] A comparative overview of the characteristics of different propulsion technologies used for a multirotor and their impact on the application areas are presented within [16, 22].

[4] Which is expressed in terms of the ratio $\frac{K_e^2}{R_a}$ consisting of the motor back-electromotive force constant K_e^2 and the equivalent resistance R_a.

[5] For more information about analysing the handling qualities of multirotor eVTOL vehicles it is referred to [26, 27] and [28].

Preferential parameters	Controllability	Handling Quality	Noise
Vehicle moment of inertia	Low	-	-
Type of rotor control	*	Pc + Sc	Pc
Number of rotors	*	-	Low
Rotor arrangement	Sym.	-	Avoid coaxial
Thrust coefficient	High	-	-
Lever arm of rotors	High	-	-
Air density	High	-	-
Rotor radius	High	*	-
Inertia of rotor	*	Low	-
Inertia of motor	-	Low	-
Inertia of gearbox	-	Low	-
Gear ratio	-	Opt.	-
Motor back-EMF	-	High	-
Equivalent motor resistance	-	Low	-
Friction	-	Low	-
Disc loading	-	-	Low
Propulsion technology	-	-	E

* No distinct statement possible, due to varying impact depending on additional parameters
Pc Rotor pitch control
Sc Rotor speed control
Sym Symmetrical
Opt. Optimized for highest motor efficiency
E Full electric propuslion system

Fig. 2 Overview of some selected beneficial parameter values and specifications in order to improve controllability, handling quality and lower noise emissions. The parameters may be dependent on each other and the list is not exclusive

1. At first, the propulsion system context is defined, which identifies external elements interacting with the propulsion system. The type of interaction is defined by the interfaces.
2. Then the use cases for the propulsion system are established and the tasks of each system context element for each use case are defined. This allows to identify all tasks and functions that need to be fulfilled by the propulsion system.
3. For each derived function, an activity diagram is developed to describe the activities that are taking place within the propulsion system itself.
4. With this information, an initial system concept is derived by grouping the identified activities and allocating them to a specific system. In accordance with Darmstadt et al. [14], the propulsion system architecture is generally composed of the following system groups:
   - Flight control system
   - Power and drive system
   - Electrical system
   - Thermal management system (TMS)

   The flight control system encompasses all sensors and systems that collect air data, receive and process control commands and calculate the corresponding motor control inputs for each motor controller for speed-controlled rotors or inputs for the actuation system of collective pitch-controlled rotors. The power and drive system (also called powertrain and drivetrain) is responsible for converting the electrical power, which is supplied by the electrical system, into mechanical rotational power in accordance with the inputs received from the flight control system. The drivetrain is a system group within the powertrain and does only include the systems that transmit the mechanical power of the engine into thrust at the rotors. The electrical system takes over the function to store and distribute the electrical energy. The thermal management system shall ensure to keep all system components within their operating temperature range. These system groups can provide an initial guidance during the architecture developing process.
5. In the last step, the propulsion concept is integrated into the complete vehicle system architecture concept and an initial sizing loop is conducted to size the eVTOL vehicle as well as the propulsion system, estimate the required power and energy and calculate the estimated weight proportions using the method presented by Bertram et al. [16]).

2.4 Safety and reliability analysis

The basis for the safety analysis is the safety and reliability requirements of EASA SC-VTOL [12] and the EASA SC E-19 [19]. With the initial understanding about the intended propulsion system components from the previous section, the safety analysis helps to identify weak points of the propulsion system and to define the type and amount of required safety measures. Thereby, system requirements for each propulsion system component can be derived which may significantly impact the propulsion system design compared to the initial design. Consequently, a more precise prediction about the required system components and their specifications can be generated.

Generally, the safety analysis for the propulsion system design is conducted using the methods described in SAE ARP4754A [18] and ARP4761 [17]. In Fig. 3, an extract of the safety assessment process is shown. The green parts mark the steps of the safety assessment that are covered within this work. In order to conduct the aircraft level Functional Hazard Analysis (FHA), the system concept from the previous section as well as a functional breakdown analysis on the aircraft level are required, which are assigned to the

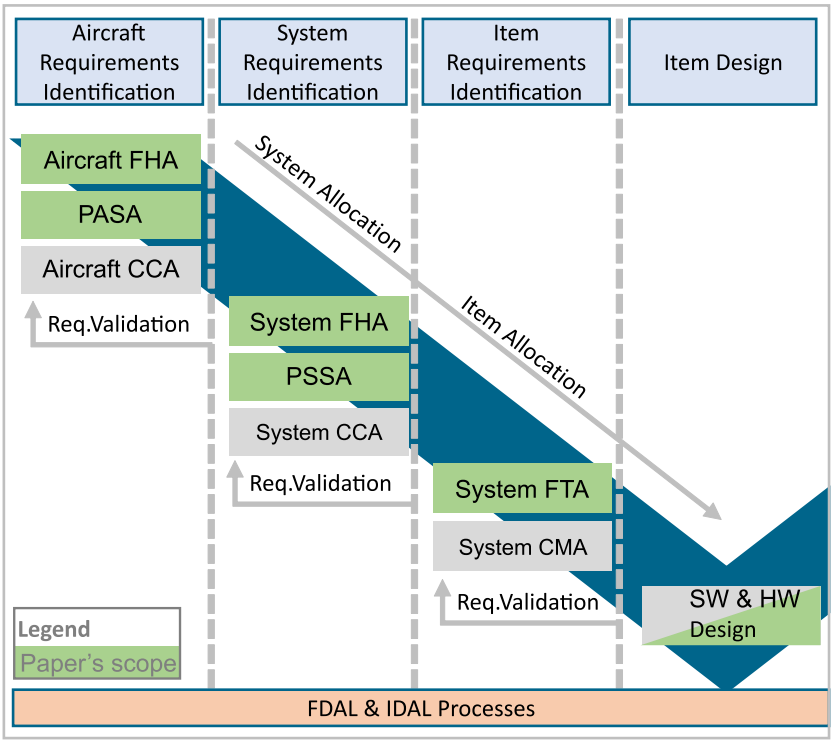

Fig. 3 Extract of the ARP4754A [18] and illustration of the safety assessment steps covered within this work (marked in green)

system development process within the ARP4754A. However, as this aircraft level functional analysis has yet not been addressed, it is herein conducted under the topic of the safety analysis. Thereafter, the aircraft level Fault Tree Analysis (FTA), the system level Functional Hazard Analysis (FHA) and FTA are conducted while iteratively gathering the information for the Preliminary System Safety Assessment (PSSA) and Preliminary Aircraft Safety Assessment (PASA) during the system design adjustments. During each iteration of the design process, the granularity of the considered systems within the safety analysis can be increased.

Consequently, a functional breakdown is being conducted to identify the main aircraft functions. In this context, especially those functions that are taken over by the propulsion system are of special interest. In the next step, an FHA is being conducted on the aircraft level which identifies the failure cases of the previous functions and their effects on, for example, the aircraft, the passengers, the vehicle and the environment. As proposed in Schäfer et al. [34], the failure cases *total loss of function*, *partial loss of function*, *unannunciated loss of function*, *incorrect operation of function*, *inadvertent operation of function* and *unable to stop the function* should be analysed and their failure effects on the aircraft be described.

The failure effect of a functional failure is the basis for the following process of developing a safe system architecture as indicated in Fig. 4. Based on the failure effect and the required Function Development Assurance Level (FDAL) as defined within the EASA SC-VTOL, an allowable failure probability is assigned to each functional failure case (label 1 within Fig. 4). For each identified functional failure case, a subsequent fault tree is created within the FTA on aircraft level to identify the causes (base events) that contribute to each functional failure case, the so-called top event (label 2). Based on the allowable failure probability for each failure case, an allowable failure probability can be assigned to each failure cause (label 3).

Up to this point, the analysis has been conducted based on the aircraft functions. In the next step, the system level is analysed by identifying the systems that contribute in fulfilling a specific aircraft function. The initial system architecture from section 2.3 is the basis for this analysis and needs to be crosschecked against all safety requirements that were derived from the aforementioned process (label 1-3). The crosscheck is done by developing a system level FTA, in which the top event of the system level FTA is the base event of the previously created aircraft level FTA. Within this system level FTA, the component failure causes leading towards the top event are collected (label 4) and their failure probabilities defined using historical data as provided by e.g. the Nonelectronic Parts Reliability Data (NPRD) Dataset [35] (label 5). With this information, the actual failure probability of a system function is calculated bottom-up (label 6) and gathered within the PASA. This process is repeated and the propulsion system architecture is adjusted until the allowable system reliability is assured by the designed propulsion system architecture. Finally, the results are collected within the PSSA, which indicates if the requirements of the aircraft level FHA can be fulfilled.

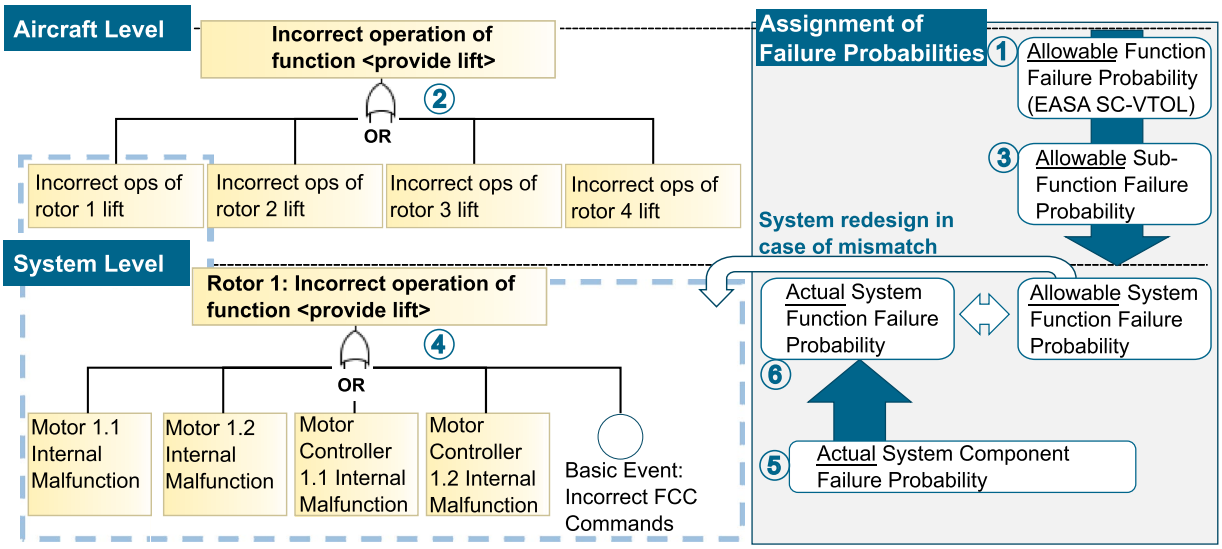

Fig. 4 Schematic depiction of the interconnection between aircraft level FTA and system level FTA

To evaluate the sensitivity of the propulsion system architecture to critical system components, minimal cut sets are generated based on Reliability Block Diagrams (RBDs) and fed back into the system design.

As the propulsion system is a safety-critical system, whose failure may cause human injury or even loss of life, the system shall only have two states: operational or failed-safe [36]. A fail-unsafe condition shall be prevented by all means. Therefore, either the design principle of a safe life or fault-tolerant design must be applied for developing the propulsion system. While a safe life design is characterized by oversizing and prematurely replacing components before failure, a fault-tolerant design requires to incorporate hardware, information, time or software redundancy [36]. The following strategies are promoted herein to ensure a safe system design depending on the analysed aircraft functional failure case:

- **Total loss or partial loss of function**:
  Implement additional system components with the same functionality (for example: passive, active or hybrid hardware redundancy).
- **Unannunciated loss of function**:
  Make use of software redundancy by implementing fault detection and fault indication mechanisms.
- **Incorrect operation, inadvertent operation, unable to stop a function**:
  Implement options for masking a faulty system component.

2.5 Propulsion system component sizing and validation

The last step within the applied propulsion system design methodology aims at further specifying the propulsion system components and validating the system architecture by sizing and simulating each component based on off-the-shelf components. The sizing is conducted using common sizing methods.[6] It is important to note that the propulsion system sizing must be connected with the whole vehicle sizing and is conducted until convergence within all vehicle components is reached. When the MTOM limit from the ConOps definition is reached or no convergence can be achieved, the sizing must be interrupted and the design must be revised. The subsequent simulation of the propulsion system helps validate if the derived vehicle architecture can suitably fulfil the initial ConOps definition and requirements. If necessary, additional architecture adjustments and requirements are derived based on the sizing and simulation results.

3 Case study

Within this section, the previously described conceptual design method is applied to a case study to derive a conceptual propulsion architecture for a battery-powered multirotor eVTOL vehicle that is operated by a pilot.

[6] For detailed information about the sizing process of a multirotor propulsion system, it is referred to Bertram et al. [16].

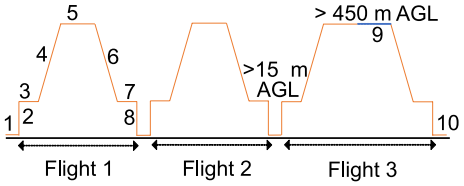

Fig. 5 Flight mission profile of the analysed use case consisting of three consecutive flights with the flight segments 1: Taxi out, 2: Vertical climb to 50ft AGL, 3: Transition to cruise, 4: Cruise climb to cruise altitude, 5: Cruise until destination, 6: Cruise descent, 7: Re-transition to hover, 8: Vertical descent to ground, 9: Diversion to alternate, 10: Taxi in. [16]

Table 1 General requirements of the ConOps definition

Parameter	Value
Flight Mission	Three Flights + 20 min Loiter
Design Range	50 km
Payload	360 kg (4 Passengers incl. Pilot)
MTOM	< 3175 kg
Vehicle configuration	Multirotor
Powertrain technology	All-electric
Energy source	Battery

3.1 ConOps definition and vehicle requirement analysis

The ConOps analysis by Asmer et al. [37] identified five potential use cases for urban air mobility vehicles: Intra-City, Airport-Shuttle, Sub-Urban and Inter-City. For this case study, the vehicle under investigation shall be operating within the Intra-City use case. The total flight mission within this use case is indicated in Fig. 5 and consists of in total 50 km, which are separated in three flights to allow for passenger embarkation and disembarkation and includes additional 20 min reserve time at minimum drag speed. The use case is further defined by transporting in total 4 passengers with 90 kg each, which results in a payload requirement of 360 kg. Additionally, the maximum takeoff mass of the vehicle is limited by the EASA SC-VTOL requirement to a maximum of 3175 kg [12]. Based on the use case analysis of [37], a multirotor vehicle is suggested to be best suited for this kind of operation. For the interest of this paper, this multirotor vehicle propulsion system shall be battery-powered. An overview of the summarized ConOps requirements is given in Table 1, in which the flight mission, payload, type of eVTOL vehicle and the powertrain technology are defined.

Up to date, the quadcopter is the most critical vehicle configuration in terms of safety as described within section 1.2 as well as energy consumption, the quadcopter vehicle configuration shall be selected for fulfilling this mission.

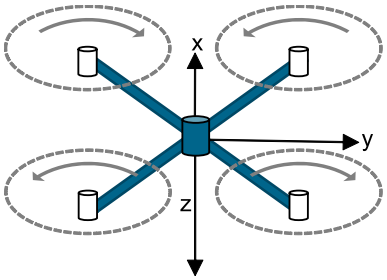

Fig. 6 Quadcopter rotor cross-configuration

Thereby, a cross-configuration of the rotors is selected, in which they are evenly and symmetrically distributed along the x- and y-axis to provide good controllability and handling quality as shown in Fig. 6. The rotors shall be fixed-pitch and speed-controlled as they promise less system complexity, even though the pitch rotor control would be beneficial in terms of controllability, achieving quick vehicle response times and low noise. The powertrain shall be all-electric and powered by batteries, since it could be shown in Bertram et al. [16] that a battery full electric powertrain is competitive compared to other powertrain technologies for up to 50 km design range, based on the current state of the art.

Controllability analysis, handling quality, and noise aspects presented within Sect. 2.2 have been taken into consideration in parallel to any system design adjustments. As they are not in focus of this paper, they are not further elaborated on herein.

3.2 Propulsion system concept definition

With the information about the ConOps and the vehicle requirements, an initial propulsion system concept is defined within step three of the applied conceptual design method. To develop the propulsion system concept, the CAMEO Systems Modeler was used. As described in Sect. 2.3, initially the system context for the system of interest is defined as shown in Fig. 7.

The system context indicates that the propulsion system of the multirotor receives control commands from the cockpit crew. These control commands are merged with data from the air data sensors in order to lift and control the aircraft for passenger transport. In order to provide, a closed control loop for the unit controlling the vehicle, currently a cockpit crew, status information is fed back to the cockpit indication systems. During the transformation of the input signals into lift and thrust, air, thermal energy and noise are interchanged between the environment and the propulsion system. As the propulsion system components will suffer of degradation during daily operation, the means for maintenance actions are included within the system context.

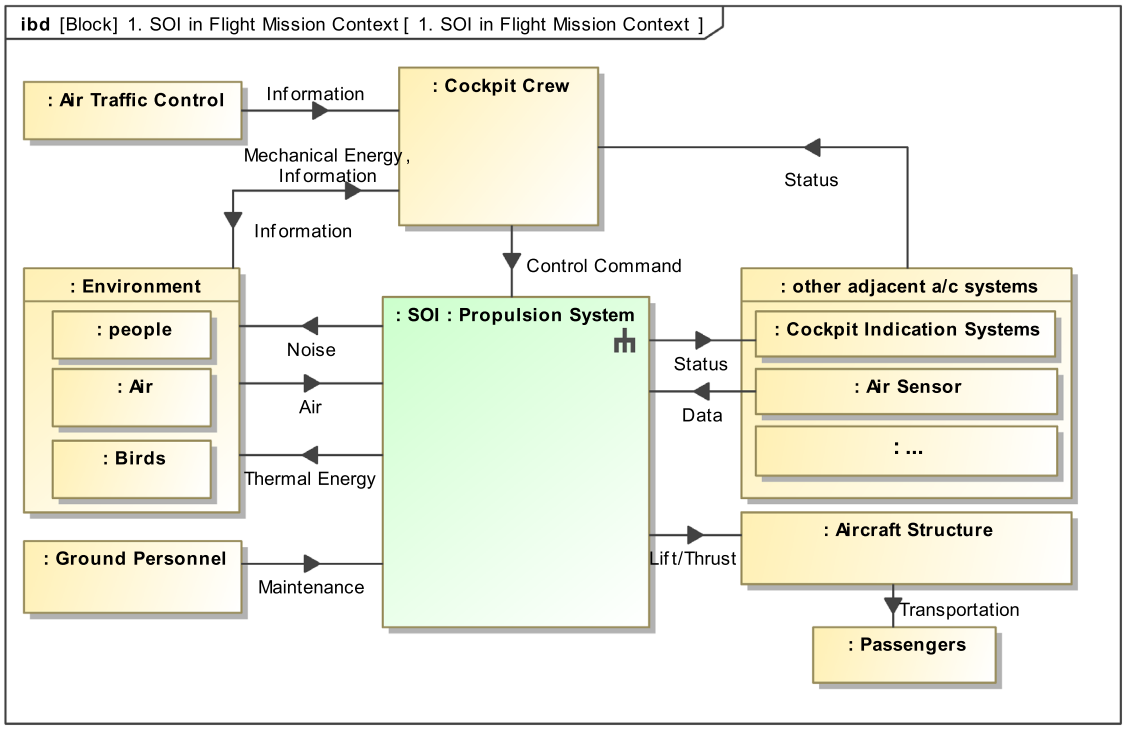

Fig. 7 System context definition for the propulsion system

By analysing the use cases of the propulsion system, numerous main functions could be identified that need to be fulfilled by the propulsion system and the adjacent aircraft systems. The activity diagrams for each identified main function enabled to identify the sub-functions for the propulsion system. Figure 24 gives an overview of all identified functions.

When grouping similar functions together, they can be allocated to respective system groups as shown in Fig. 25. It becomes apparent that the four generic system groups, namely the flight control, the power and drive, the electrical and the thermal management system group, as described in Sect. 2.3, can be identified here as well. In addition to that, the functional analysis requires the integration of an information system group into the propulsion system as it is essential to feed back the information from all participating propulsion system groups back to the cockpit and an optional in-service monitoring unit for health monitoring and improving maintenance schedules. Besides the identification of the main system groups, this graphical representation allows to identify the item flow between the different system groups. Within the next step of the architecture development, each functional block is assigned to a specific system component as shown in Fig. 26 and, thereby, an initial logical propulsion system architecture is developed. Within this architecture, the flight control system group is composed of at least a Flight Control Computer (FCC) and an air data computer gathering and distributing air sensor data including GPS data. Using the control inputs from the cockpit and the air data, the FCC calculates and controls the required power setting for the electric motor and thereby regulates also the corresponding setting of the thermal management system. The power and drive system group consists of motor controllers, motors, optionally gearboxes and the rotor. The energy for the power and drive system group is provided by electrical system group which consists of the battery system, a power distribution system and battery control units. The information system group consists of data concentrator units which gather and distribute status information. The thermal management system is not further specified, as its system requirements are unknown so far. However, based on the sizing and simulation of the power and electrical system group within Sect. 3.4.1, some specifications for an thermal management system are collected in Sect. 3.4.3. Merging this logical architecture with the other vehicle systems as described within Sect. 2.3, an initial sizing loop for the whole vehicle system is conducted. However, as this is not part of this paper, it is referred to [16].

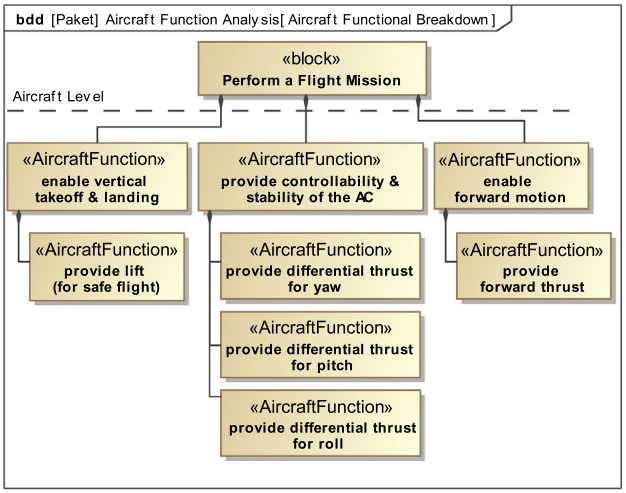

Fig. 8 Functional Breakdown analysis with the aircraft functions that are connected to the propulsion system

Within the subsequent safety analysis, the propulsion architecture is further modified to fulfil the safety requirements of EASA SC-VTOL [12] of the enhanced[7] vehicle category. The considered systems within the safety analysis are indicated in Fig. 26. However, for simplification reasons, the thermal management system and the information system group are initially excluded from the safety assessment and will be integrated in the future.

3.3 Safety and reliability analysis

The safety and reliability analysis as presented in Sect. 2.4 has been conducted using the SysML Modelling Language within the CAMEO Systems Modeler together with the SysML Profile Risk Analysis and Assessment Modelling Language (RAAML) [38] and the FHA profile [34] which facilitate conducting a model-based safety assessment. The safety analysis loop has been run through several times during the design process to account for the system changes that were required to reach the reliability guidelines and to account for the results of the sizing process. Therefore, the following section presents the main results of each step of the safety analysis based on the final propulsion system architecture as presented in Sect. 3.5.

Functional Breakdown Analysis Within the functional breakdown analysis, the main aircraft level functions were identified that are taken over by the propulsion system as shown in Fig. 8:

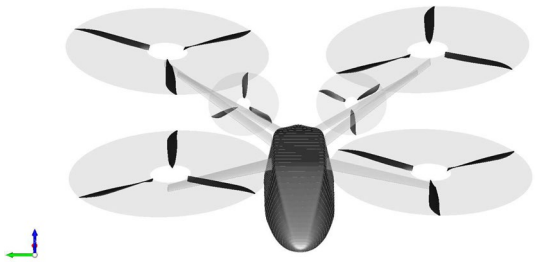

Fig. 9 Visualization of the quadcopter with two push propellers [27]

1. provide lift for safe flight,
2. provide differential thrust for yaw,
3. provide differential thrust for pitch,
4. provide differential thrust for roll and
5. provide forward thrust.

Functional Hazard Analysis During the initial safety analysis loop, it became quickly apparent that a quadcopter with a non-redundant propulsion system as presented in previous section[8] will require so many additional redundancies that the design will most probably not be reasonable in terms of total weight and system complexity. The difficulty of the quadcopter configuration is that a partial loss of providing lift may be caused, for example, by a single rotor failure which exhibits a failure probability of $2.83 \cdot 10^{-4}$ per hour.[9] The *partial loss* of providing lift caused by a single rotor failure within a quadcopter configuration must be expected to be a catastrophic event [13] which shall not happen more often than $1.0 \cdot 10^{-9}$ per hour as it is categorized as a FDAL A event within EASA SC-VTOL [12]. Therefore, a main vehicle design adjustment was conducted by adding two push propellers to the rear of the vehicle as shown in Fig. 9.

This measure assumes that the resulting yaw moment of one rotor loss can be counteracted and the failure effect of a partial loss of providing lift caused by one single main rotor loss attenuates from a catastrophic event to a hazardous event with an allowable failure probability of $1.0 \cdot 10^{-7}$ per flight hour and less redundancies can be expected to be required.

An aggregated overview of the FHA results based on this quadcopter configuration with two push propellers is given in Table 2. Especially the failure cases *total loss* or *partial loss* of a function as well as the *inadvertent, incorrect operation* including the *unable to stop* functional failure are

[7] As soon as the vehicle is expected to transport passengers over congested areas, it falls into the certification category enhanced of EASA SC-VTOL with the highest required safety levels.

[8] During the first iteration, a quadcopter vehicle configuration is assumed in which each rotor is powered by a pure series connection of the system components FCC, battery, motor controller and electric motor as described in the previous Sect. 3.2.

[9] This failure rate results when using the component failure rates presented later on in Table 3.

Table 2 FHA failure effect classification for each identified aircraft level function

Function failure	Provide lift	Provide diff. thrust for pitch	Provide diff. thrust for roll	Provide diff. thrust for yaw	Forward thrust
Total loss	catastrophic	catastrophic	catastrophic	hazardous	major
Partial loss	hazardous	hazardous	hazardous	n.a	n.a
Incorrect ops	catastrophic	catastrophic	catastrophic	hazardous	catastrophic
Inadvertent ops	catastrophic	catastrophic	catastrophic	hazardous	catastrophic
Unable to stop	catastrophic	catastrophic	catastrophic	hazardous	catastrophic
Unsym. partial loss	n.a	n.a	n.a	minor	minor
Degradation	major	major	minor	minor	minor

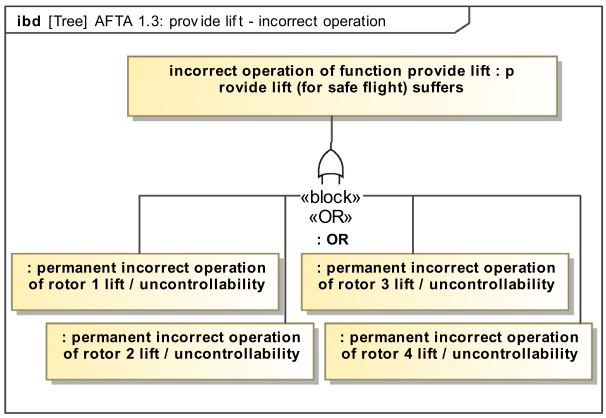

Fig. 10 Aircraft FTA for the functional hazard "Incorrect operation of the function: provide lift"

critical for the system design since they exhibit catastrophic or hazardous events. For all functions that have at least a catastrophic and hazardous failure effect, the corresponding Aircraft FTA is being conducted.

Aircraft level FTA Results The Aircraft FTA for the catastrophic event *incorrect operation* of the function <provide lift> is presented exemplarily in Fig. 10.

As the permanent incorrect operation of the function to provide lift is classified as a catastrophic event with an allowable failure probability of $1.0 \cdot 10^{-9}$ per hour, it can be concluded that the permanent incorrect operation of one rotor is allowed to happen with a probability lower than $2.5 \cdot 10^{-10}$ per flight hour. With this information, the system architecture that propels each rotor is designed in the next step using the system level FTA. By developing all FTAs for the catastrophic failure effects of the aircraft functions, it becomes apparent that, according to the herein used definition, the inadvertent operation or unable to stop functional failures are subsets of the incorrect operation. Therefore, three main basic events remain that need to be further analysed within the system level FTA:

- Total loss of one rotor lift
- Incorrect ops of one rotor providing lift
- Incorrect or inadvertent ops of one propeller providing thrust

System level FTA results

On the system level, the rotor drive system architecture is revised until the *total* loss and the *incorrect ops* of one rotor fulfils the failure probability goals defined within the aircraft level FTAs of $< 2.5 \cdot 10^{-8}$ and $< 2.5 \cdot 10^{-10}$ respectively. Using a single drive unit without any redundancies and assuming conservative failure probabilities as listed

Table 3 Failure rate probability for each propulsion system component

	Component	Failure condition	Applied Failure Rate[1]
BAT	Battery	Failure	$9.31 \cdot 10^{-5}$ [35]
MC	Motor Controller	Failure	$4.75 \cdot 10^{-5}$ [13]
M	Electric Motor	Failure	$9.24 \cdot 10^{-5}$ [13]
GB	Gearbox	Failure	$5.00 \cdot 10^{-6}$ [13]
FCC	Flight Control Computer	Failure, Malfunction	$1.57 \cdot 10^{-5}$ [35]
REL	Disconnect Power Relay	Unintended opening, Failure to operate	$4.60 \cdot 10^{-5}$ [35]
DISC	Disconnect Clutch	Unintended opening, Failure to operate	$4.70 \cdot 10^{-5}$ [35]

[1]Due to lack of data it is assumed that the applied failure rate is the same for the different failure conditions. The failure rate for each component was chosen rather conservative. Further explanatory information concerning the applied failure rates are provided in the Appendix B: Failure Rate Background Information

Table 4 Extract of the PSSA results showing the expected system failure rates for the most limiting system level FTA top events

Functional Hazard	Max. allowable failure rate	Expected failure rate
Loss of one rotor lift	$< 2.5E-8$	$1,06 \cdot 10^{-8}$
Inadvertent ops of one rotor	$< 1.0E-9$	$2.37\ 10^{-20}$
Incorrect ops of one rotor	$< 2.5E-10$	$2.46 \cdot 10^{-10}$
Inadvertent ops of one propeller	$< 5.0E-10$	$2.76 \cdot 10^{-15}$

in Table 3, the *total loss* of one rotor must be expected to occur with a probability of $2.8 \cdot 10^{-4}$. Therefore, as a first countermeasure, the rotor drive is designed as a dual active drive system composed of two drive units. As the dual active drive system would still exhibit a failure rate for a *total loss* of one rotor of $5.6 \cdot 10^{-8}$, each motor controller unit shall be powered by at least two separate battery packs and a dual active / passive channel motor controller shall be used. The passive channel continuously monitors the main motor controller and shall be able to take over its function (hot standby redundant system).

For meeting the maximum allowable failure rate for the *incorrect operation* of one rotor, it is essential to reduce the probability that an erroneous FCC signal, motor controller output or motor output propagates up to the rotor. First, the probability of an erroneous motor controller output is already reduced by the use of a dual channel motor controller. Second, it must be prevented that any malfunction within the electric motor is passed to the rotor. Therefore, two masking strategies must be in place: once by disconnecting the power from the electric motor using an emergency power disconnect relay and second using a mechanical disconnect clutch that separates the motor output from the rotor shaft. Third, the probability of an erroneous or missing valid FCC command is reduced by implementing a triple modular redundant FCC setup which enables determination of the correct output by majority voting. Each FCC is then required to exhibit a malfunction or failure probability of less than $1.58 \cdot 10^{-5}$ per hour.[10] By implementing these strategies, both the probability for an erroneous power output of the driving units and the FCC group are reduced below 10^{-10} per flight hour which reduces the *incorrect operation* of one rotor to $2.46 \cdot 10^{-10}$ and therefore fulfils the allowable failure probability. The system FTA with the identified system components of the final propulsion system architecture contributing to a permanent *incorrect operation* is shown in Fig. 27. The *incorrect* or *inadvertent operation* of the rear push propellers can be mitigated by the use of triple redundant FCC signals, a dual channel motor controller and a single disconnect option, like a disconnect relay.

To also identify common causes of error, minimal cut sets were calculated and analysed within a reliability block diagram analysis. All derived requirements from the system level FTA and the minimal cut sets are listed below. Implementing these requirements for the overall system architecture ensures that the maximum allowable failure rates for the four system level FTA top events or respectively the basic events of the aircraft level FTA as shown in Table 4 can be complied with.

1. Each rotor requires a dual active redundant drive train. When a geared propulsion is chosen each drive train must also be equipped with a separate gearbox.
2. Each rotor unit must be able to produce ≥ 50 % of the total vehicle thrust required for hover for a prolonged time.
3. For a short time interval, each rotor unit must be able to produce more than 50 % of the total hover thrust (ideal would be to provide ≥ 50 % of the total vertical climb thrust) in order to break any vertical descent during landing.
4. Each motor unit must be able to be passivated and therefore be equipped with at least two means of decoupling, preferably a mechanical and electrical decoupling device.
5. Any internal fault of the motor control units must not lead to an unrecognized malfunction that propagates to the electric motor. Therefore, the motor control units should be designed as dual channel active passive units.
6. The passive channel of the motor control unit acts as a fail-safe-backup mode that activates in case of any loss of input signal from the FCCs or in case of a motor control unit malfunction. In this state, the motor control unit should command a constant motor rotational speed which corresponds to the hover state in normal flight.
7. Each motor control unit must be connected to at least two batteries or power supply busses to achieve a dual modular redundant power source. To prevent any common cause failures in total, at least 4 battery packs are required for the four main rotors and one additional separate battery pack is required for the rear push power train.
8. One independent stand-alone battery source must be used to power both push-propeller units together.
9. Both rear propellers in combination must be able to create a vehicle yaw moment bigger than the result-

[10] Based on the NPRD, this requirement is expected to be realistic as control board failure probabilities in average exhibit a failure rate of $1.2 \cdot 10^{-6}$ per hour [35], which therefore still allows for considering a deduction factor of 10 due to stresses that are caused by environmental influences and the operation.

Table 5 Extract of the PASA results showing the expected failure rates for each identified catastrophic aircraft level function

Function failure	Provide lift	Provide diff. thrust for pitch	Provide diff. thrust for roll	Provide diff. thrust for yaw	Forward thrust
Total loss	$4.49 \cdot 10^{-16}$	$4.49 \cdot 10^{-16}$	$4.49 \cdot 10^{-16}$	Hazardous	Major
Partial loss	$4.24 \cdot 10^{-8}$	$4.24 \cdot 10^{-8}$	$4.24 \cdot 10^{-8}$	n.a	n.a
Incorrect ops	$9.86 \cdot 10^{-10}$	$9.86 \cdot 10^{-10}$	$9.86 \cdot 10^{-10}$	Hazardous	$5.52 \cdot 10^{-15}$
Inadvertent ops	$9.86 \cdot 10^{-10}$	$9.86 \cdot 10^{-10}$	$9.86 \cdot 10^{-10}$	Hazardous	$5.52 \cdot 10^{-15}$
Unable to stop	$9.86 \cdot 10^{-10}$	$9.86 \cdot 10^{-10}$	$9.86 \cdot 10^{-10}$	Hazardous	$5.52 \cdot 10^{-15}$
Unsym. partial loss	n.a	n.a	n.a	Minor	Minor
Degradation	Major	Major	Minor	Minor	Minor

ing yaw moment of two shutdown concordant rotating main rotors.

10. The FCC setup must be triple modular redundant using majority voting. Each FCC must exhibit a failure rate of $\leq 1.58 \cdot 10^{-5}$ per hour

It becomes apparent that the loss of one rotor lift and the incorrect operation of one rotor providing lift are the most critical system design drivers for the propulsion system of the main rotors. As soon as the failure rate requirements are fulfilled for those events, the other functional hazards will be fulfilled as well. The push-propeller architecture however, is mainly driven by the functional hazard of an inadvertent operation of each propeller.

The resulting achievable failure rates for the top events of the aircraft level FTA, which were identified within the FHA, are summarized in Table 5. It is important to note that the architecture design and its failure probabilities are based on the following assumptions:

1. The loss of one main rotor does not lead to a catastrophic event as the opposite main rotor will be shut down to achieve equilibrium in pitch and roll. The resulting yaw moment is counteracted by the push propellers at the rear. The quadcopter therefore remains controllable and is able to continue safe flight and landing.
2. Each motor can be passivated by an own electric disconnect relay as well as a mechanical declutch mechanism. Thereby, it is assumed that for passivating the electric motor it is sufficient if either the mechanical declutch or the electric disconnect relay is activated. However, the control logic will only allow recovery of the electric motor drive to power the rotor if both the mechanical and electrical switches are closed. This is required in order to prevent a passivated malfunctioning electric motor drive to become operative due to an inadvertently closed electrical switch or mechanical clutch.
3. The propulsion system components do not exhibit higher failure rates as assumed within Table 3. Adverse operating conditions, high thermal and electrical stresses might increase the actual failure rates and eventually require a modification of the proposed propulsion system architecture to account for more redundancy. A continuous condition monitoring should be implemented to identify those adverse condition and near term failure conditions.

3.4 Propulsion system component sizing and validation

Within this section, the main system groups of the propulsion system are sized, compared with off-the-shelf components and additionally simulated. At first, the power and drive system is specified. Based on these results, on the one hand, the electrical system group with a primary focus on the batteries and on the other hand the thermal management system for the propulsion system are developed and analysed. The simulation for each system group was carried out using the open modelling language Modelica within the Dymola environment by Dassault Systèmes. Therein, all propulsion system components were analysed based on their published specifications. Any degradation effects such as increased friction within the electric motor and gearbox or reduced capacity and increased internal resistance of the battery cells, are currently not implemented.

3.4.1 Sizing and simulation power system

As the power and drive system group consists of the motor controller, the electric motor, the gearbox and the rotor (see Fig. 26), this section presents the specifications of these components for the main rotor and the rear push propeller drive system. The results are based on the following assumptions[11]:

1. The main rotor drive is designed for a maximum rotor tip speed of $Ma_{tip} = 0.45$ during normal operation and two rotor blades to ensure a quiet operation. The disc load-

[11] They are based on the results of previous preliminary parameter studies presented within Bertram et al. [16] and Atci et al. [26, 27].

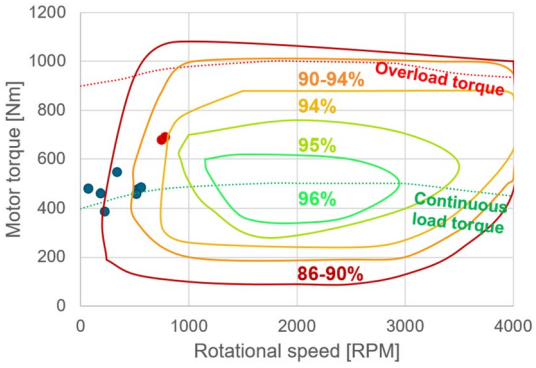

Fig. 11 Representation of the electric motor operating points for a direct drive architecture (blue: hover, vertical climb, cruise climb, cruise, loiter, vertical descent; red: emergency hover and vertical climb) fitted within the efficiency map of a commercial off-the-shelf motor [40] that is providing up to 1000 Nm torque

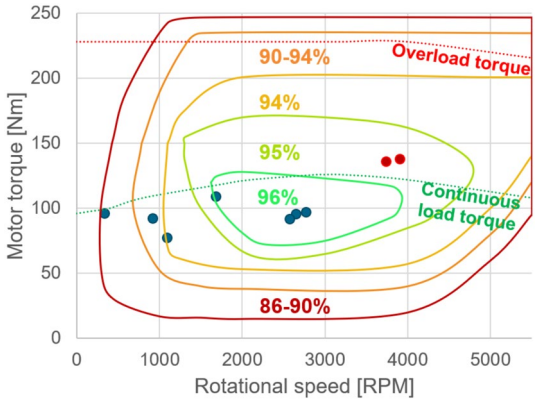

Fig. 12 Representation of the electric motor operating points for a geared drive architecture with a 5:1 gear reduction ratio (blue: hover, vertical climb, cruise climb, cruise, loiter, vertical descent; red: emergency hover and vertical climb) fitted within the efficiency map of a commercial off-the-shelf motor [41] that is providing up to 230 *Nm* torque

ing of 200 N/m^2 is chosen to aim for an energy efficient flight and minimise rotor losses.

2. The rear push propeller is designed for a cruise tip speed of $Ma_{tip} = 0.5$, using a propeller with two blades and a propeller radius of 0.54 m to provide a cruise speed of 110 km/h at 3120 RPM.
3. The system voltage for the power and drive system components is defined with 600 V.[12]

Based on the safety assessment, a total power of at least 200 % compared to the highest continuous required flight power needs to be provided by the four main rotor drives. For the quadcopter configuration, this amounts to at least 450 kW that needs to be provided by eight electric motors.

During the sizing process, a direct drive architecture was compared to a geared drive for the main rotor propulsion architecture. The comparison of a direct drive and a geared drive architecture assuming commercial off-the-shelf permanent magnet synchronous electric motors (PMSM) and planetary gearboxes[13] clearly indicates the disadvantages of a direct drive. The currently available electric PMSMs cannot be operated in their optimal efficiency range due to the low rotating speeds and high torque values that are required for the quadcopter main rotor propulsion. The efficiency of the direct drive lies between 85 % and 92 % as indicated in Fig. 11, whereas the geared drive is able to operate between 92 % and 96 % as indicated in Fig. 12. Therefore, higher thermal heat losses must be suspected using a direct drive.[14]

In terms of the main propulsion system weight (consisting of the electric motor, motor controller and gearbox), the geared propulsion architecture exhibits a weight of 374 kg compared to 400 kg for the direct drive. As it can be seen in Fig. 13, the weight of the direct drive powertrain is mainly driven by the electric motor. While the electric motor for the geared powertrain is approximately 70 % lighter, heavy gearboxes are required to provide sufficient torque capability. Still, a weight saving of almost 7 % is estimated using the geared drive.

This comparison of the motor efficiency and the expected propulsion system weight shows that the usage of a geared drive is advisable to save weight and thermal losses. The gearbox as an additional component of the powertrain therefore needs to be considered in the safety and reliability analysis.

The propulsion system for the rear push propulsors is sized to provide the highest efficiency during the cruise flight. This requires an electric motor to provide the highest efficiency at 3120 RPM and 99 Nm torque. In total, the electric motors for the rear push drive are expected to weigh 42 kg and amount to 58 % of the rear propulsion weight. As the rear drive system does not require a gearbox, the motor controllers make up for the remaining 42 %.

[12] The specification of 600 V is a trade between firstly low currents with less heat losses, lower cable weights, smaller power electronic components, higher efficiencies, second available off-the-shelf propulsion components and third the risk of partial uncontrolled discharges and arcing. The same voltage level is defined for the electric power system of the eVTOL by Joby Aero, Inc. [39]. However, those voltage levels pose challenges regarding wire insulation, filtering, EMI shielding, and require high reliability drive components combined with health management concepts [14].

[13] Based on an internal market study, suitable commercial off-the-shelf products were selected for this comparison.

[14] Further information about the thermal management system are provided in the chapter 3.4.3.

Table 6 Recommended specifications for the power system components of the main rotor

Component	Specification
Specifications of the main rotor power and drive system:	
Electric Motor	• Highest efficiency at 500-550 RPM (without gearbox) or 2650-2800 RPM (gearbox 5:1) with 100 Nm torque (hover & vertical climb operating point)
	• Continuous torque capability of ≥ 120 Nm and ≥ 145 Nm maximum peak torque
	• Continuous power capability of 29 kW and a maximum peak power of 58 kW
	• Max RPM at ≥ 780 RPM (without gearbox) or 3905 RPM (with gearbox 5:1)
Gearbox	• Reduction gear ratio of 5:1
	• Input rotating speed range of 330-2770 RPM (normal ops), up to 3905 RPM in irregular operation
	• Output rotating speed range 66-554 RPM (normal ops), up to 781 RPM in irregular operation
	• Equivalent output torque of ≥ 455 Nm
	• Maximum peak output torque of ≥ 700 Nm
Motor Controller	• Continuous power of ≥ 30 kW
	• Maximum peak power of ≥61 kW
Specifications of the push propeller power and drive system:	
Electric Motor	• Highest efficiency at 3120 RPM with 99 Nm torque (cruise operating point)
	• Continuous torque capability of 99 Nm and a maximum peak torque of 125 Nm
	• Continuous power capability of 32 kW and a maximum power of 60 kW
	• Max RPM of ≥ 4576 RPM
Motor Controller	• Continuous power of ≥ 34 kW and maximum peak power of ≥ 63 kW
	• Continuous motor current ≥ 90 A and maximum motor current ≥ 108 A

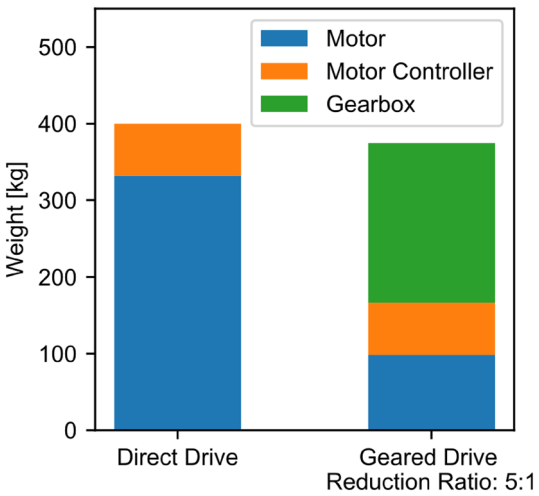

Fig. 13 Weight comparison of a direct drive and geared propulsion system for the main rotor

The specifications for each component of the main rotor and rear propeller power and drive system are listed in Table 6. Degradation effects of the electric motor, gearbox and motor controller might alter the achievable performance of the vehicle over time.[15] However, it is assumed, that regular maintenance intervals and their corresponding maintenance actions can prevent the degradation effect of those components becoming noticeable.

The simulation of the power and drive system has shown that the powertrain components with the above-mentioned specifications are suitably sized for powering the main rotors as well as the push propellers. Also, in failure conditions, the main rotors can still be accelerated to the required rotational speeds. The preliminary dynamic simulation of the rotor rotational speed following control signals shows rise times in the magnitude of tenth of seconds, depending on the step size. However, whether or not this rise time of the rotor is sufficient to achieve quick response times of the total vehicle and therefore to achieve good handling qualities is still under further analysis.[16]

Based on these analyses, the following implication can be drawn for the propulsion system architecture: Using a gearbox is recommended for the main rotor drive system.

[15] The electric motor as well as the gearbox typically experience an increase in friction due to contamination, corrosion or deficient lubrication of the bearings which can eventually lead to bearing damages, higher power requirements and reduced flight performance Nandi et al. [42]. The second most often motor failures are insulation defects caused by thermal stress which can lead to stator armature and ultimately motor failures Nandi et al. [42].

[16] For further information concerning the controllability and handling quality of RPM controlled rotors within a quadcopter it is referred to [27].

Table 7 Allocation of the four main battery packs to the motor controllers of each main rotor drive system

	Rotor 1	Rotor 2	Rotor 3	Rotor 4
MC x.1	BAT 1	BAT 1	BAT 3	BAT 2
MC x.1 ALT	BAT 3	BAT 2	BAT 2	BAT 3
MC x.2	BAT 2	BAT 3	BAT 4	BAT 4
MC x.2 ALT	BAT 4	BAT 4	BAT 1	BAT 1

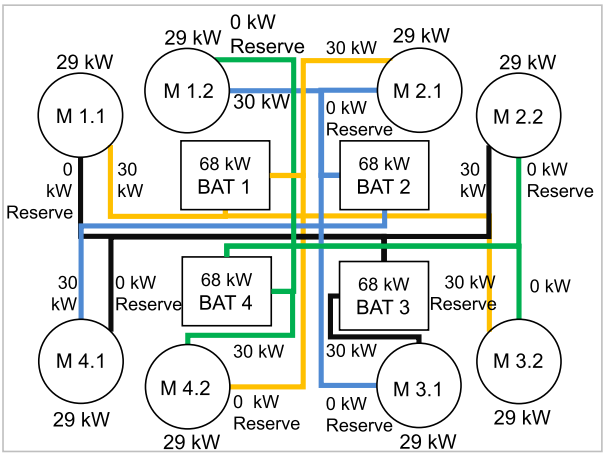

Fig. 14 Power allocation of the main rotor battery packs during normal operation. Above or below each motor symbol, the maximum required power of each electric motor is indicated for the shown operating state. The required motor controller power is shown next to the corresponding power lines of the motor symbol. On top of each battery pack, the maximum available power of each battery pack is listed

3.4.2 Sizing and simulation electrical system

Based on the functional propulsion architecture of Fig. 25 and the correspondingly derived logical architecture of Fig. 26, a battery storage system is required to power the propulsion system. As described by the requirement no. 7 of the system and reliability analysis of Sect. 3.3, in total four identical batteries are required for powering the main rotors and one common battery pack is required for the rear push-propeller drive trains. Within this section, an initial sizing of the energy storage system is conducted. This includes an analysis of the required energy, the battery pack size and weight by considering failure conditions of the propulsion system during flight.

Looking into the electrical power distribution of the main rotors, each motor controller needs to be able to receive power from an alternate battery source in case its main battery source is unavailable, in order to fulfil the requirement of Sect. 3.3. Therefore, an allocation as shown in Table 7 is chosen. The table indicates that for the rotor drive number 1, the motor controller 1.1. receives mainly power from battery 1 but can be switched to battery 3, whereas motor controller 1.2 is powered by battery 2 and 4. Based on this allocation, each battery continuously powers two motor controllers, with each motor controller consuming a maximum of 30 kW during normal operations.

Figure 14 shows the power allocation of the main rotor battery packs during normal operation.

Based on the allocation, the sizing of the battery packs can be conducted which is influenced by the following requirements:

1. The batteries must provide the total energy required for fulfilling the flight mission during normal ops
2. The capacity of each battery pack must be sufficient to provide sufficient power for the connected motor controllers during normal ops
3. The battery packs must provide enough energy and power for enabling a continued safe flight and landing during any failure condition

Each requirement is now analysed separately. As a basis, the Panasonic 18650 lithium nickel–manganese–cobalt (NCA) battery cells are used [43] and cell degradation effects are excluded. Since a system voltage U_{sys} of 600 V is chosen, each battery pack should provide 600 V which requires 167 cells connected in series.

Battery sizing based on the required total energy and power for normal operation:

Based on the energy requirement of 19.7 kWh[17] for powering two drive units during normal operation for the total flight mission E_{BS}, the required battery pack capacity $C_{BP,E}$ amounts to 32.8 Ah.

$$C_{BP,E} = \frac{E_{BP}}{U_{sys}} = \frac{19.7\ kWh}{600\ V} = 32.8\ Ah$$

The battery capacity based on the two supplied drive units with a required maximum power P_{max} of 30 kW each for normal operations amounts to 29.3 Ah.

$$C_{BP,P} = \frac{P_{max}}{\xi \cdot U_{sys}} = \frac{2 \cdot\ 30\ kW}{3.448\frac{1}{h} \cdot 600\ V} = 29.3\ Ah$$

using the cell discharge rate ξ that is composed of the Panasonic rated battery cell current i_{Batt} and rated capacitance c_{Nenn}

[17] The energy requirement was derived from the initial sizing process and validated with the developed simulation model.

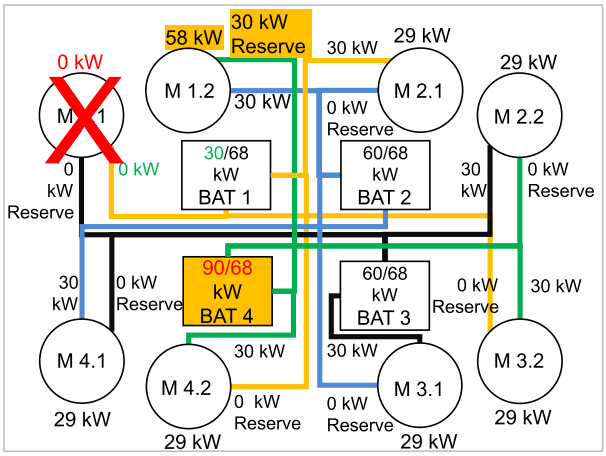

(a) Failure case: single rotor drive unit loss caused by a motor or motor controller failure (not optimized)

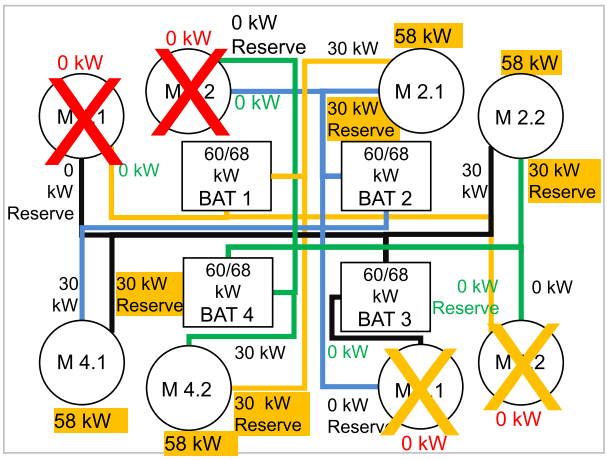

(b) Failure case: complete main rotor drive loss

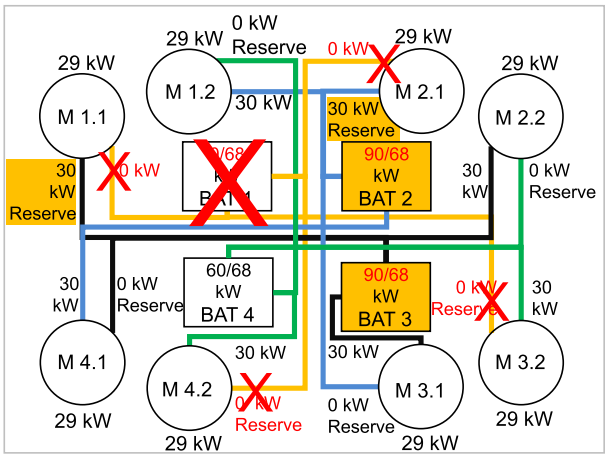

(c) Failure case: single battery pack loss

Fig. 15 Power distribution of the main rotor battery packs for different failure cases

$$\xi = \frac{i_{Batt}}{c_{Nenn}} = \frac{10\ A}{2.9\ Ah} = 3.448 \frac{1}{h}.$$

Sizing the battery with the higher of both capacity requirements of 32.8 Ah results in a battery pack that is able to provide 68 kW discharge power.

$$\begin{aligned} P_{available} &= C_{BP} \cdot \xi \cdot U_{Sys} \\ &= 32.8\ Ah \cdot 3.448\ \frac{1}{h} \cdot\ 600\ V \\ &= 68\ kW. \end{aligned}$$

Battery sizing based on the energy and power requirement during failure conditions.

The three most restrictive failure conditions are analysed and their effects on the power distribution of the battery packs shown in Fig. 15:

- Failure of one rotor drive unit due to motor or motor controller unit failure
- Failure of one rotor unit
- Failure of one battery pack

Power requirement: During a single motor unit loss or a failure of one battery pack, at least one of the remaining battery packs is required to supply at least 90 kW power as indicated in Fig. 15a and 15c. In order to provide 90 kW battery pack power, a pack capacity of 43.5 Ah is required.

$$C_{BS,P} = \frac{P_{min}}{\xi \cdot U_{sys}} = \frac{90\ kW}{3.448 \frac{1}{h} \cdot 600\ V} = 43.5\ Ah$$

During a single rotor loss, however, the available 68 kW pack power is sufficient to cope with this failure.

Energy requirement: Whether or not the battery capacity is sufficient for reaching a suitable airfield even during failure conditions depends on the type of failure condition, the time at which the failure occurs and the intended emergency flight procedure. Herein the most unfavourable conditions are assumed:

- Based on the previous failure analysis the type of failure condition is assumed to draw 90 kW power of a single battery pack for the remainder of the flight.
- The failure condition occurs on the third flight of the total flight mission at the equal time point (ETP).[18] The ETP for the defined flight is reached 5.7 min after start of the third flight segment. Up to this point, approximately 12.2 kWh are already consumed, which includes

[18] The ETP defines the point within each flight, where the time to reach the next suitable airfield equals the time to return to last overflown or departed airfield.

Table 8 Summarized capacity requirements for each main rotor battery pack based on the energy and power requirements

Capacity Requirement based on	Battery capacity	Destination reachable?[1]
Energy required (normal ops)	32.8 Ah	no
Energy required (emergency ops)	34.3 Ah	yes[2]
Power required (normal ops)	29.3 Ah	no
Power required (emergency ops)	43.5 Ah	yes

[1] Indicates whether destination can be reached in case of emergency operation starting within the third flight segment

[2] Defines the absolute minimum

Table 9 Summarized capacity requirements for the push propulsion battery pack based on the energy and power requirements

Capacity Requirement based on	Battery capacity	Destination reachable?[1]
Energy required (normal ops)	70.0 Ah	no
Energy required (emergency ops)	88.8 Ah	yes [2]
Power required (normal ops)	32.6 Ah	no
Power required (emergency ops)	61.1 Ah	no

[1]Indicates whether destination can be reached in case of emergency operation starting within the third flight segment

[2]Defines the absolute minimum

the energy for flight one and two and the energy up to the ETP.[19]

- There is no other closer landing site available than the intended destination. Therefore, the flight is continued to the destination.

With these assumptions, another 8.5 kWh is required, which is the equivalent energy to reach the destination airfield within 5.7 min. Therefore, a battery capacity of at least 34.3 Ah or 20.6 kWh are required. All battery pack capacity requirements of the normal and failure condition operation are summed up in Table 8.

It becomes apparent that a main rotor battery pack capacity of 43.5 Ah is required and driven by the maximum power requirement during the failure condition caused by a single rotor drive unit loss or a battery pack loss. Under normal operating conditions, a pack with this capacity will be discharged down to 25 % after having completed the flight mission and used 20 min reserve flight time and will have 9.2 min of flight time available at the occurrence of a failure condition at the ETP during the third flight. A battery with these specifications can be composed of 15 of the Panasonic cells connected in parallel and 167 in series, so that in total 2505 cells[20] are used. Each battery pack then weighs 120 kg.

Battery sizing for the rear push propulsion system:

The same assessment is conducted for the push propeller propulsion battery pack, which must be able to provide at least 68 kW power during normal operation and 126 kW power during an emergency condition at which a main rotor has failed. The results are summarized in Table 9.

The battery pack capacity in this case is mainly driven by the energy requirement during the failure condition at the most unfavourable point of time. Therefore, the battery is sized with a capacity of at least 88.8 Ah[21] respectively 54.1 kWh, which results in having 31 parallel cells and 167 cells connected in series. In total, 5177 cells are required, which results in a capacity of 90 Ah, with 186 kW available power. During normal operation, the battery pack is discharged down to 37 % in case the 20 min loiter time had been utilized during flight. At the ETP, the battery provides enough energy to power the push propulsion system for another 6 min in case of emergency operations, which is sufficient to reach the landing site. Further optimization of the battery pack size could be gained by an intelligent battery management system that allows an interconnection between all battery packs and, thereby allocates energy and power requirements smartly between all battery packs. The simulation of the battery packs in combination with the previous power and drive system has indicated that the battery is sufficiently sized to provide energy for the whole flight mission.

As this analysis assumes non-degraded battery cells, the cyclic and calendar day aging of the cells will negatively impact their capacity and increase their internal resistance [44]. According to literature, it must be suspected that the battery capacity will degrade by 14 %–16 % after 200 to 400 cycles depending on the usage [45].[22] Additionally, the increase in internal resistance will adversely affect the available power. As both, the main and rear battery packs are

[19] Assuming the flights one and two were carried out as planned and no contingency energy has been used.

[20] The effect of battery degradation has so far not been in the scope of this research.

[21] As the battery sizing based on the normal operation results in more than 20 % less required capacity than based on the highest failure case capacity requirement, no additional reserve of 20 % for the battery capacity is included.

[22] Further information about the calculation of battery degradation can be found at [44].

sized according to the emergency operation requirements, the normal operation will not be affected by this amount of degradation. However, the main battery packs must be expected to deliver less than the required emergency power and the rear battery pack will not be able to provide enough energy to cover the remaining flight distance from the ETP to the final destination during emergency operation. In order to account for the degradation effect, all packs would need to be oversized by about 20 %, which would also lead to an increase in system weight of about 20 %. This indicates, how important it is to closely monitor the battery health during operation.

Within the next section, the heat development within each battery pack is analysed and the requirements for a cooling system are identified.

Summary of the derived specifications for the propulsion architecture:

- Each main rotor battery pack requires a battery capacity of at least 43.5 Ah and should be able to provide at least 90 kW power.
- The push-propeller battery pack requires a battery capacity of at least 88.8 Ah and should be able to provide at least 68 kW power.
- An additional capacity reserve of about 20 % might be necessary in order to fulfill the emergency operation requirements also with a degraded battery pack.

3.4.3 Sizing and simulation thermal management system

Within this section, the results of the heat development simulation within the power and drive system components are presented and initial system requirements for a thermal management system derived. As a result from previous section, this analysis is based on the propulsion design which incorporates a geared drive propulsion system, whereas the gearbox, as an encapsulated system, can be expected to be self-cooling and lubricating, the electric motor and motor controller are expected to be combinable within a cooling system due to their similar requirements. For the battery packs, however, a separate thermal management system is expected to be required, which provides heating at low temperatures and cooling during operation at high operating temperatures to keep the batteries within their optimal operating temperature range of 20–40 °C.[23] When assuming

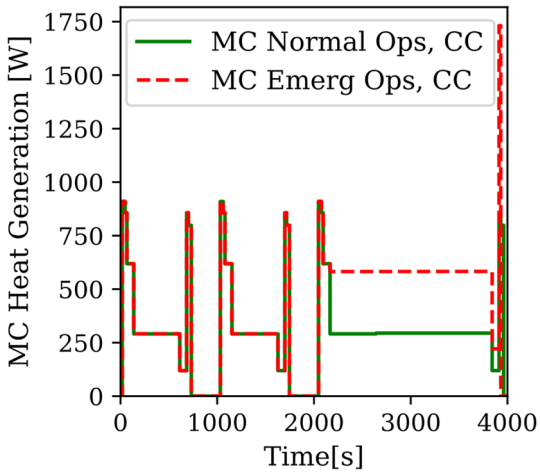

Fig. 16 Heat generation of the electric motor during normal and emergency operation which is assumed to start at the end of the vertical flight phase of the third flight

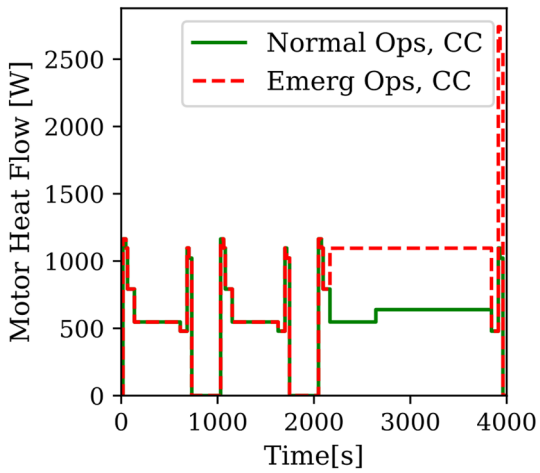

Fig. 17 Heat generation of the motor controller during normal and emergency operation which is assumed to start at the end of the vertical flight phase of the third flight

VTOL operation at the warmest areas within Europe, ambient temperatures of up to 42.7 °C[24] are taken into account during the design process of the propulsion and cooling system.

Initially the thermal management system requirements for the motor and motor controller of one rotor drive system are evaluated. Analysing the amount of generated heat within the electric motor and motor controller gives the following results. During the phase of the highest power requirement,

[23] Higher battery temperatures might be possible, as some studies allow the battery to heat up to 80 °C [46]. However, in order to minimize, the thermal runaway hazard of NCA cells Duh et al. [47] recommend to keep lithium-ion batteries below 60 °C. In order to additionally maximize the battery lifetime, Vedachalam and Vandavasi [48] even advise to keep the battery cells between 20 and 30 °C. Consequently, within this study, a conservative temperature range of 20–40 °C is used, which is comparable to the design of Darmstadt et al. [13], enhances safety and prolongs battery lifetime.

[24] This value corresponds to the highest measured temperature of the European city Madrid within the years 2017 and 2022 [49].

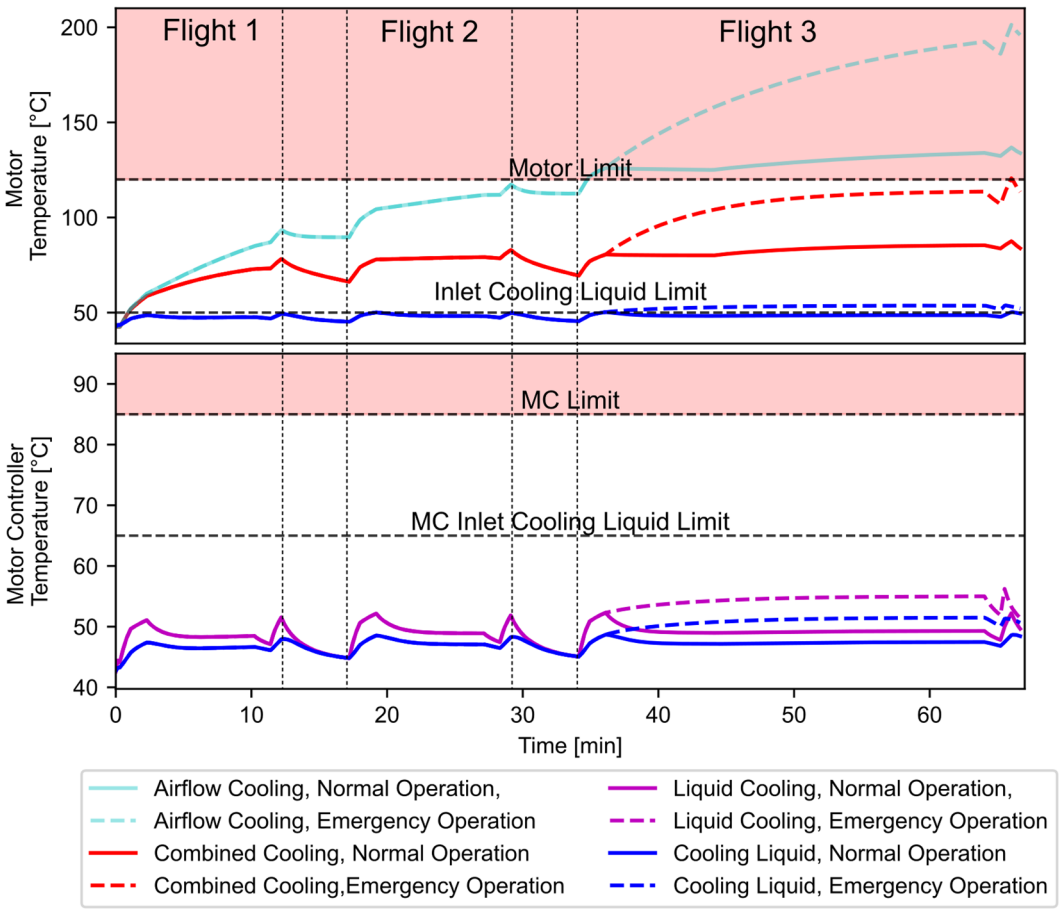

Fig. 18 Temperature development within the electric motor copper windings using only air flow cooling (AF) or a combined cooling (CC) compared to the temperature development of the motor controller using liquid cooling

the vertical climb phase, the motor controller and the electric motor are expected to produce up to 1.1 kW and 1.4 kW heat respectively under normal operating conditions as shown in Fig. 16 and 17. During emergency conditions, in which only one electric motor is left driving a main rotor, the heat output amounts to 1.8 kW and 2.9 kW respectively.

As the intended electric motor provides means for airflow cooling, its effect on the heat development within the electric motor components is initially analysed. With an ambient air flow that is based on the flight mission, the flight speeds, the vehicle rotor configuration and the cooling tubes geometry, the temperature within the copper windings of the electric motor will still rise over 120 °C during the transition of hover to cruise climb of the third flight within the flight mission after 2088 s and reach a maximum of 136 °C as shown in Fig. 18. Thus, the temperatures within the electric motor cannot be kept below 120 °C during normal operation using only the ambient air flow. Operating in the emergency rating, in which one electric motor must provide the full power for a single rotor, the temperatures within the electric motor would even rise over 200 °C during the third flight of the mission (see Fig. 18). Consequently, the electric motor cooling system must be complemented by an additional liquid cooling system. As the analysed motor controller also requires liquid cooling according to the manufacturer's data sheet in order to keep its temperature below 85 °C, the motor controllers and corresponding electric motors of one rotor drive unit are combined within the same liquid cooling system. As the four rotor drive units will be located below each rotor and therefore be located distant to each other, a separate cooling system for each rotor drive unit is recommended.

As a conclusion, the following requirements must be fulfilled by a combined ambient air flow and liquid cooling system for the off-the-shelf analysed electric motor and motor controllers.

1. The electric motor operating temperature must be kept below 120 °C also during emergency conditions while the motor is operating in emergency rating.

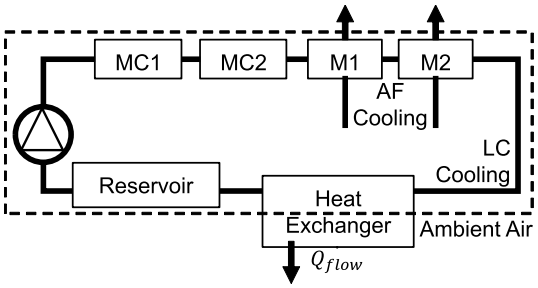

Fig. 19 Schematic view of the combined cooling system for the electric motor and motor controller consisting of a liquid cooling cycle and airflow cooling

2. The motor controller operating temperature must be kept below 85 °C during all operating conditions (normal and emergency rating).
3. As the motor controller can be operated with a liquid cooling temperature of a maximum of 65 °C and the electric motor requires liquid cooling temperatures below 50 °C, the thermal management system needs to keep the cooling liquid temperature below 65 °C when passing the motor controller and 50 °C when passing the electric motors.
4. The maximum volume flow of cooling liquid for the motor controller is 6-12 l/min, whereas the electric motor can only withstand 6-8 l/min.
5. The maximum input pressure of the liquid cooling shall not exceed 2 bar when entering each electric motor.

One exemplary cooling topology that is able to fulfil these requirements consists of the motor controllers and electric motors of each rotor being connected in series as shown in Fig. 19. As the motor controllers can withstand higher liquid input pressures and emit less heat, they are placed at the beginning of the cooling flow. The electric motors can then be placed downstream.[25]

The combined cooling system (CC) consisting of airflow cooling (AF) and liquid cooling (LC) is designed with the following specifications:

- Cooling fluid: Glysantin G40
- Cooling liquid flow: 0.14 kg/s
- Cooling air flow: dependent on flight phase—maximum available 2.3 m^3/kg
- Heat exchanger size: 0.3 · 0.3 · 0.3 m
- Heat exchanger weight: 3.8 kg

[25] A possible alternative would be to place the electric motors in parallel downstream.

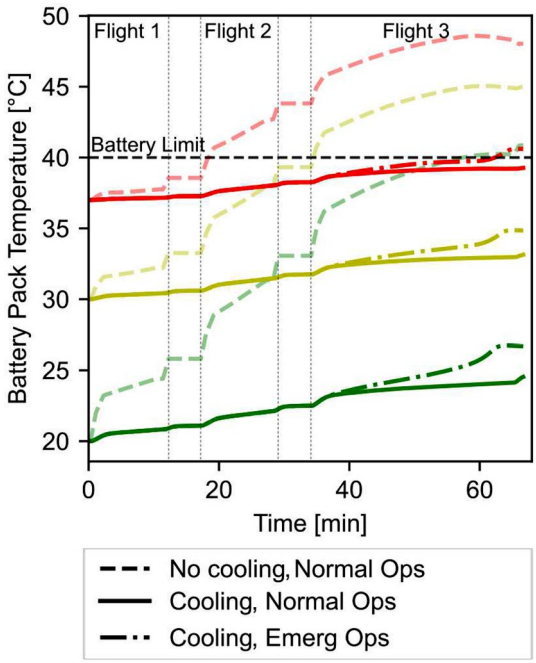

Fig. 20 Temperature development within each battery pack at different ambient temperatures (green lines: 20 °C, yellow lines: 30 °C, red lines: 37 °C) with and without cooling during normal operation

The temperature development within the electric motor using this cooling topology of combined cooling for the electric motor and liquid cooling for the motor controller are shown in Fig. 18. It can be seen, that the temperature within the electric motor stays below 120 °C during all operating conditions, even in emergency conditions at the most unfavourable situation during the flight mission when using a combined liquid and air-cooling system. Figure 21 indicates how the generated heat within the electric motor is absorbed by the ambient air flow and the liquid flow. As not all of the generated heat within the first flight can be dissipated, the temperature within the electric motor components rises during the flight mission. The inlet liquid cooling temperature for the electric motor as shown in Fig. 18, however, almost reaches the maximum manufacturer's recommendation of 50 °C during normal operation. Operating in emergency rating the inlet temperature even rises up to 54 °C and therefore exceeds the manufacturer's limit of 50 °C.

The temperature within the motor controller stays well below its limit of 85 °C as shown in Fig. 18. All of the heat is absorbed by the liquid cooling flow. During the whole flight mission, the maximum inlet temperature of the liquid fluid for the second downstream motor controller (MC2) reaches a maximum of 60 °C (during emergency ops) and therefore stays below the required 65 °C.

To prevent an excessive heat build-up during the ground phases of the flight mission, in which the vehicle is not moving and therefore receives no cooling air flow, it is essential

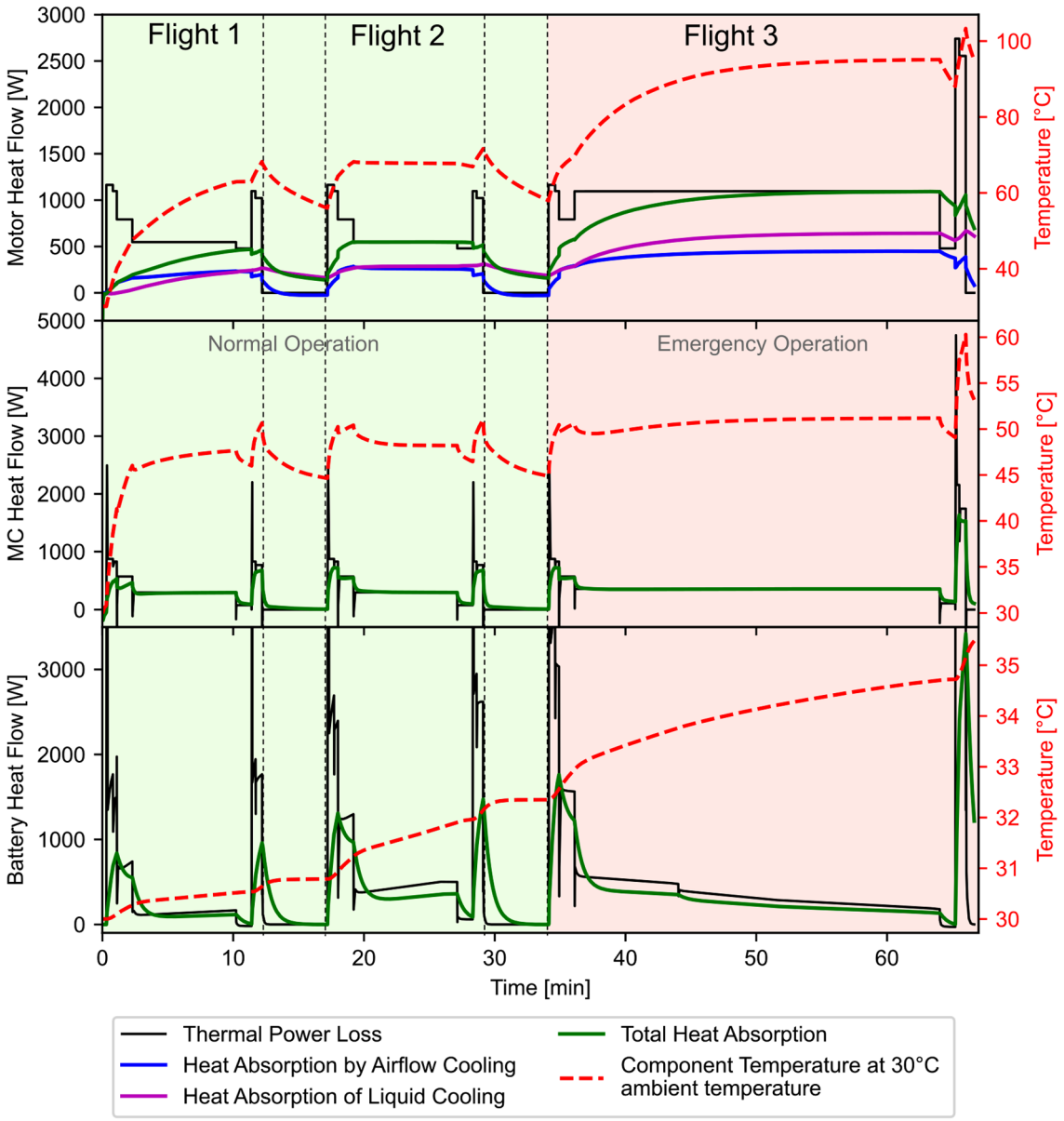

Fig. 21 Heat power loss within the electric motor, motor controller and battery pack and its dissipation via ambient air flow and / or liquid cooling at an ambient temperature of 30 °C during normal operation (green background) and emergency operation (red background)

to keep up the liquid cooling flow as well as the cooling air flow. Therefore, the liquid cooling pump needs to be operative. Additionally, a ground fan, should be installed to facilitate the heat transfer within the heat exchanger. Using no ground cooling, the temperature of all components within the cooling system would heat up to over 65 °C during the five minutes ground phase. The same effect can be observed after termination of the flight mission, where a temperature of 77 °C can be observed across all components after 30 min. By increasing the ground cooling time up to 30 min the overall temperature can be kept below 50 °C.

In the following, the thermal management system requirements for the battery packs are evaluated, based on the power that is drawn by the power and drive system.[26] Fig. 20 compares the temperature development within each battery pack during normal operation with and without any cooling system. It becomes clearly visible that the batteries cannot be operated without a cooling system as the battery

[26] The power drawn by the thermal management system is currently not considered, but should be analysed and eventually be integrated in future studies.

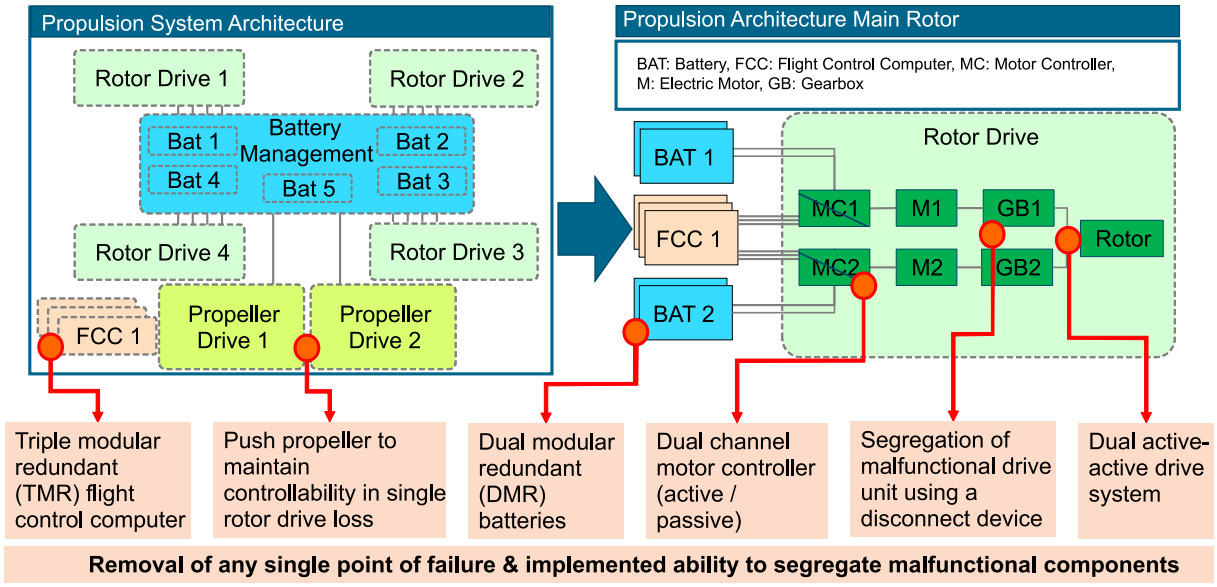

Fig. 22 Schematic representation of the overall quadcopter propulsion architecture and its implemented safety measures, excluding the thermal management system

pack temperature will exceed the 40 °C temperatures limit even at 20 °C ambient temperatures. Using a liquid cooling circuit with a glycol–water mixture of 20:80 that is channelled along each battery cell, the temperatures of each battery pack can be kept below 40 °C during normal operation if the ambient temperature does not rise above 37 °C. However, under emergency operation, in which one battery pack has failed during the transition to cruise on the third flight segment, the battery pack temperature of two battery packs (refer to Fig. 15c) will even increase up to 40.6 °C at ambient temperatures of 37 °C. The ambient temperature has to stay below 36.2 °C in order to ensure a battery pack temperature below 40 °C during emergency conditions using a liquid cooling circuit. The liquid cooling circuit used within this simulation has the following properties:

- Outer cooling circuit—ambient air volume flow: 0.3 m^3/s
- Inner cooling circuit—liquid volume flow: $6.8 \cdot 10^{-5}\ m^3/s$
- Inner cooling fluid: glycol–water mixture 20:80

For higher ambient temperatures, a refrigeration cycle is required which is part of future research.

A summarizing overview about the expected behaviour of the electric motors, motor controllers and main rotor battery packs as well as their thermal management systems during normal and emergency operation is given in Fig. 21. Besides the expected heat flow also, the amount of heat absorption of each used cooling method is shown. Additionally, the temperature development of each component is indicated for a typical hot summer day with 30 °C ambient temperature.

Based on the analyses of this section, the following implications can be drawn for the propulsion system architecture:

1. Each propulsor requires a separate cooling system
2. For each electric motor, that was chosen and analysed herein, a combination of liquid cooling and air cooling is required as only air cooling is not sufficient to cool the electric motor sufficiently.
3. Each motor controller requires a liquid cooling system
4. The motor controller and electric motor can be cooled using the same liquid cooling system.
5. Each liquid cooling system consists of the components: pump, cooling fluid reservoir, heat exchanger.
6. The cooling system should stay operative after each flight on ground for up to 30 min to prevent the cooling liquid to exceed the motor inlet temperature of 50 °C and to absorb the stored thermal energy within the electric motor and motor controller.
7. The battery needs an own thermal management system that is capable of cooling and heating. If operating at ambient temperatures of 20–36.2 °C, each battery pack can be cooled using a liquid cooling cycle. For ambient temperatures outside this range, the thermal management system still needs to be analysed and designed.

Table 10 Summary of the propulsion system weights

	Weight per Unit [kg]	Total Weight [kg]
Main rotor propulsion system[1]	24.6 + 17 + 52	98.4 + 68 + 208
Push propulsion system [2]	12.3 + 8.5	24.6 + 17
Battery packs [2]	120 + 248	480 + 248
Total propulsion system		1144

[1] Weights indicated for motor weight, motor controller weight and gearbox weight

[2] Main battery pack and push drive battery pack

Power distribution system and cooling system currently excluded from weight analysis

3.5 Final architecture

This section presents how the requirements of the previous sections were implemented in the final propulsion system design. This architecture is expected to fulfil the safety reliability requirements. A schematic representation of the propulsion system architecture for the quadcopter is shown in Fig. 22. On the left side, the main propulsion systems are shown with the four main rotor drives that are supplemented by two push drives. Each drive unit is connected with the battery units. In total, at least three FCC are provided. On the right, the propulsion architecture for each main rotor is depicted in more detail. It shows that the main rotor propulsion architecture is composed of two electric motors that drive the rotor through two separate gearboxes. Each motor is driven by its own motor controller, while each motor controller is backed up with a passive control board that takes over, in case faulty signals are sent by the primary controller or even the connection is lost. Each motor controller receives power from one of the four main batteries and can be switched to an alternate battery source if necessary. Additionally, each motor controller receives inputs from all three FCC and determines the valid FCC input by majority voting. The main criticality of the propulsion system of the push-propeller drive is the *incorrect operation* including the *inadvertent* or *unable to stop operation* which are classified as a potentially catastrophic event. To prevent the inadvertent operation, the motor controller fail-safe operation as already introduced for the main rotor propulsion system is implemented as well as an option for passivating a faulty motor output by implementing a power disconnect switch. The integration of a thermal management system and the information management system has been excluded so far, but will be included in further research.

Based on the sizing of all components, the total propulsion system weight for the presented multirotor excluding the thermal management systems is expected to reach 1144 kg as shown in Table 10. An overview about further vehicle design parameters can be found within Table 11 of the appendix A.

4 Conclusion and final evaluation

Within this paper, initially a method was presented for the conceptual design of an eVTOL propulsion system. This method was then applied to a multirotor vehicle for a specific intracity use case, with a special focus on developing a safe propulsion architecture, sizing each component and validating the architecture by simulation. In the following, the results are structured to answer the initial research questions:

How should the conceptual design process of the propulsion system be carried out for an all-electric multirotor VTOL vehicle that is transporting passengers so that the safety goals of EASA SC-VTOL can be met?

The conceptual design method as presented within Sect. 2 is divided in five steps. Within step one, the concept of operation needs to be defined, which includes defining the flight mission and payload requirements. Based on these requirements, the vehicle configuration has to be preselected and the powertrain technology to be used is defined. Within step two, several further requirements are developed which are based on the required controllability, the handling quality and allowed noise emission. Within the third step, the propulsion system is defined which can be segregated into defining the flight control system, the power and drive system, the electrical system and the thermal management system considering the previously established requirements. This propulsion system concept is then refined within the safety analysis and sized as well as validated within the vehicle sizing and simulation step. The system architecture refinement process is usually an iterative process between the concept definition, the safety analysis and the succeeding sizing step and is being conducted until the safety requirements of EASA SC-VTOL can be met.

What is the impact of the EASA SC-VTOL reliability requirements on the conceptual design of a multirotor propulsion system?

Based on the safety & reliability analysis, it became apparent that the loss of one rotor lift and the incorrect operation of one rotor providing lift are the most critical system design drivers for the propulsion system of the main rotor in terms of the reliability requirements. Additionally, it was identified that, if the failure rate requirements can be fulfilled for those events, the other functional

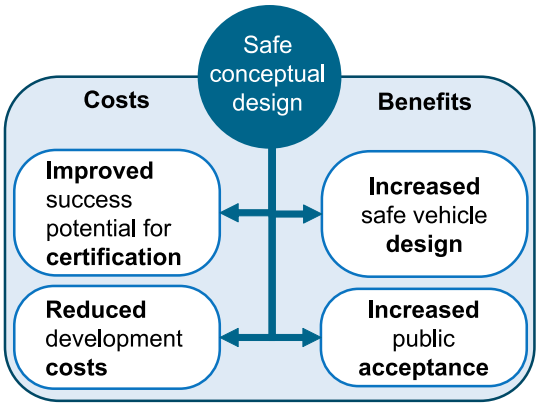

Fig. 23 Mapping the areas of the UAM overall system that are positively impacted by the presented work

hazards will be fulfilled as well. Therefore, the focus of any system designer should be put on meeting the safety & reliability requirement for the total and partial loss of one main rotor and for the incorrect operation of one rotor. Within the analysed case study, the safe propulsion system for the multirotor requires numerous redundancies. This includes that each main rotor requires two separate drive trains, which can be masked by two means in case of any malfunction within each drive train. One option for passivating the drive train is using a disconnect clutch, the other option is to cut the power to the electric motor by using a power disconnect relay. Additionally, each of the two drive trains driving the rotor must be designed for being capable to provide 200 % of normal power in case of any system malfunction. In case of a signal loss of the triple modular FCC system, each motor controller must be designed as a dual active/passive module, which is additionally equipped with a backup mode. This backup mode shall be able to set a constant rotor speed slightly below hover power for normal flight. Four battery packs are advisable to be used for the four main rotor propulsion system. Each motor controller should be connected to at least two batteries. Additionally, two push propellers are required which counteract the torque moment in case of one main rotor loss. The push-propeller architecture is mainly driven by preventing the inadvertent operation of each propulsor. Consequently, the corresponding motor controllers should be connected to the fifth stand-alone battery pack and also incorporate a fail-safe backup mode. This time one disconnect relay is sufficient for passivating faulty drive outputs. In terms of the cooling system for each main rotor drive system, it must be ensured that not more than one cooling system fail simultaneously, as the failure of the cooling system results in the loss of the corresponding main rotor. For the cooling system design of the battery packs, it must be ensured that not more than one battery pack is influenced in case of a cooling system failure. A complete loss of the cooling function may become a catastrophic event.

Which specific design and sizing characteristics must be considered for an battery-electric propulsion system architecture apart from the safety requirements?

The sizing and simulation process revealed the following implications for the propulsion system: The sizing of the power and drive system identified that a gearbox is required for driving each main rotor of the quadcopter. Only by increasing the number of rotors, the gearbox could become obsolete.

During the sizing of the battery, it became apparent that it is essential not only to check the energy and power requirement during normal operation, but also during emergency operation. The case study of this paper has shown, that the sizing of the main rotor battery packs for the presented architecture, is not driven by the energy amount or power requirement during normal operation but rather by the power requirement during emergency operation, in which two of four packs need to deliver 1.5 times the power compared to normal operation. The sizing of the push drive system battery pack is driven by the energy requirement during emergency operation which requires 1.27 times the energy for normal operation.

Which requirements must be met by a thermal management system of the developed all-electric multirotor propulsion system?

A battery-electric multirotor propulsion system requires at least two cooling circuits. The sizing of the thermal management system for the power and drive components revealed that the electric motors and the motor controllers of each drive unit can be cooled within the same liquid cooling system, whereas the battery requires a separate cooling system due to the different operating temperatures. For cooling the electric motor and motor controller, it is not sufficient to rely on the airstream. However, a combined cooling of airflow cooling and liquid cooling should be preferred. The liquid cooling circuit can cool the electric motor as well as the corresponding motor controllers of one drive unit simultaneously, by connecting them, for example, in series. This exemplary liquid cooling circuit requires at least 0.14 kg/s flow rate, using Glysantin G40. This enables to keep the electric motor below 90 °C during normal operation and just below 120 °C during emergency operations, even at ambient temperatures up to 42.7 °C. Additionally, the heat exchanger and the electric motors must be placed within the airstream to allow for additional air cooling. The heat exchanger can be expected to weight around 4 kg with a size of $0.3 \cdot 0.3 \cdot 0.3$ m. In order to cool down the heated components after each flight, it is necessary to keep the cooling system operative on ground as well. This cool-down can take up to 30 min depending on the outside temperature. A secondary liquid cooling circuit is required in order to keep the battery packs below 40 °C

operating temperature, as without any cooling circuit the batteries would heat up above 40 °C even at ambient temperatures of 20 °C. A cooling circuit using a glycol–water mixture of 20:80 with a mass flow of 0.0695 kg/s is expected to keep the operating temperature of the battery pack within $T_{amb} + 5\ °C$ during normal operation and in case of an emergency procedure within $T_{amb} + 7\ °C$. The liquid cooling system however, can only be used up to ambient temperatures of 36.2 °C. Higher ambient temperatures require a refrigeration circuit. In order to ensure a minimum battery operating temperature of 20 °C, a heating circuit is advisable as soon as the ambient temperature falls well below 20 °C.

Comparing the results to the literature identified within Sect. 1.2, specifically the research of Darmstadt et al. [14], this work presents an alternative solution for a safe propulsion system design for a quadcopter. In addition, the implications of such a propulsion system on the total propulsion system mass and a validation of the system architecture based on current technology is provided through simulation models.

5 Future perspective

Within this research, a conceptual design process for achieving a safe propulsion system for eVTOL multirotors was presented. Consequently, this work provides a first starting point for the propulsion system design which needs to be further analysed and iterated during the following detailed design phases using for example further sensitivity analysis. As the focus was set primarily on designing a reliable drive system, other system groups that are linked to the propulsion system, like the information management system, the electrical system, the thermal management system as well as safety systems need further investigation. First, the thermal management system as well as the information system group need to be included in future safety analysis. Second, the electrical system architecture, therein especially the power distribution, should be analysed in further detail. In this context, it is crucial to further investigate the feasibility of using a system voltage of 600 V and its impact on the reliability of 600 V propulsion components. As battery degradation has only been covered very briefly, further detailed analysis of its effect on the sizing of the battery packs should be conducted in the future. Third, the safety system requirements defined within the EASA SC E-19 [19] has to be included within the propulsion architecture design which includes, e.g. means to prevent and cope with uncontrolled fire within the battery system. Fourth, the rotor, rotor shaft connection as well as the junction between the two gearboxes and the rotor shaft need to be designed from a mechanical perspective and investigated to prevent single point of failures. Fifth, the thermal management system of the battery needs to be extended as the currently assumed liquid cooling circuit is only able to provide sufficient cooling below ambient temperatures of 36.4 °C. Therefore, a lightweight and safe refrigeration circuit should be assessed as an alternative. In order to ensure the correct battery operating temperature even at low ambient temperatures, adding a heating possibility to the battery pack thermal management system probably using the heat of the motor and motor controllers should be considered. Additionally, a comparative study for the liquid cooling circuit of the electric motors and motor controllers should be conducted to assess the implications of a two-step cooling instead of the currently evaluated one-step cooling system. Sixth, the heat development within the power and drive system of the rear propulsion needs to be investigated and the thermal management system adapted accordingly. As the presented propulsion architecture is only valid, if the vehicle can continue safe flight and landing even during a single rotor loss, further investigation is required to establish corresponding means of controlling such a flight state.

5.1 Contribution of this work towards minimizing costs and maximizing benefits of a UAM system

In accordance with the leitmotif "Opportunities and Challenges of Urban Air Mobility", this section evaluates how this work contributes to advancements within the Urban Air Mobility (UAM) system (see Fig. 23). The contribution in making UAM become reality can be grouped in minimizing UAM costs or maximizing UAM benefits. As this work presented a method for the conceptual safe design of the propulsion system as well as its implications on the propulsion system architecture for an exemplary UAM concept of operation, this paper primarily adds value towards increasing the reliability of a vehicle design. By providing means for a model-based systems engineering approach for the safe vehicle design, the chance of a fast and successful certification process may also be increased. Additionally, by taking safety aspects into account already during the conceptual design phase, subsequent high vehicle development costs due to late design adjustments can be prevented. On the other hand, the safe propulsion design as presented for the multirotor may positively influence the passenger's acceptance towards these vehicles.

Appendix A: Further vehicle specifications

Table 11 Summary of the HorizonUAM multirotor vehicle concept parameters

	Multirotor concept vehicle
Propulsion Type	Battery-Electric
Control Scheme	Rotor Speed Control
Design Gross Weight	1954 kg
Payload Capacity	360 kg
Number of Rotors	4
Rotor Radius	2.64 m
Max Rotor Tip Speed (Normal Ops)	M.45
Max Rotor Tip Speed (Emergency Ops)	M.65
Number of forward facing propellers	2
Propeller Radius	0.54 m
Max Propeller Tip Speed	M.54
Battery Capacity	263 Ah / 159 Wh
Design Range	3x16.7 km + 20 min Loiter

Appendix B: Failure rate background information

This subsection shall provide explanatory information regarding the assumed failure rates of the propulsion components and their effect on the presented results. In this context, the battery and motor controller are analysed in detail, as their failure rates are rather sensitive to made assumptions. To all components applies that the actual failure rate of each component may vary depending on the quality of manufacturing, deployed raw materials, manpower quality, equipment used, quality control mechanism as well as the operating conditions [48]. Consequently, as long as the specific component is not tested separately in the future operating condition, the actual failure rate will always differ from those based on literature and mathematical models.

Battery cell failure rates

In the following, the applied failure rate of $9.3 \cdot 10^{-5}$ for the NCA battery pack is put into context. The failure rate of a battery pack can be computed by $\lambda_{pack} = n \cdot \lambda_{cell}$ and is consequently dependent on the number of cells per battery pack n and the failure rate of a battery cell λ_{cell} [52]. According to Vedachalam and Vandavasi [48], λ_{cell} is influenced not only by the battery cell type but also the maintenance interval, charge–discharge cycles and the cell quality which is further influenced by the manufacturing and process quality. The most widely used battery cells with the highest specific energy density are lithium nickel–manganese–cobalt (NMC), lithium nickel–cobalt–aluminum oxide (NCA) and lithium–iron phosphate (LFP) cells. As Ohneseit

Table 12 Overview of lithium-ion battery failure rates

Context	Cell type	Cell failure rate	Pack failure rate	Reference
Multirotor lithium battery	unknown	–	$9.3 \cdot 10^{-5}$	[13, 35]
Aircraft batteries (military context)	unknown	–	$3.8 \cdot 10^{-6}$ to	[35]
		–	$3.0 \cdot 10^{-5}$	
Offshore vehicles	NMC	$3.5 \cdot 10^{-9}$ to	–	[48]
		$5.8 \cdot 10^{-9}$	–	
Boeing 787 battery	NCA	$2.5 \cdot 10^{-7}$ *	$1.2 \cdot 10^{-5}$	[50]
Light duty vehicles	all	–	$4.0 \cdot 10^{-5}$ to	[51]
			$7.6 \cdot 10^{-5}$	

et al. [53] and Duh et al. [47] identified during their analysis of the different behaviour of battery cell types, NCA cells have the highest thermal runaway hazard as they develop the highest temperature in case of a thermal runaway compared to LCO, NMC and LMO cells. The lowest hazard exhibits the LFP cells as their highest thermal runaway temperature amounts to only 260 °C and their temperature development is comparatively slow [47]. Therefore, NCA cells exhibit potentially higher failure rates as NMC and LFP cells. The failure rate is further negatively impacted when the cells are exposed to charge–discharge-cycles beyond 60 % [48], discharge rates above 2 C [52], large maintenance intervals or operating temperatures above 60 °C [47, 52].

The chosen failure rate of $9.3 \cdot 10^{-5}$ is aligned with the failure rate used within Darmstadt et al. [13] in order to achieve comparable results of the propulsion system architectures. Thereby, the failure rate already includes a factor 10 for adverse operating conditions compared to the baseline failure rate. When looking into other exemplary failure rates from the literature (see Table 12), the NPRD database provides failure rates for battery packs used in the context of military aircraft between $3.8 \cdot 10^{-6}$ and $3.0 \cdot 10^{-5}$ [35]. Vedachalam and Vandavasi [48] analysed NMC cells used in offshore service vehicles with a 3-month maintenance interval and identified a failure in time (FIT) rate between 3.1 and 5.8, which corresponds to a failure rate of $3.1 \cdot 10^{-9}$ and $5.8 \cdot 10^{-9}$. Assuming, that one battery cell failure already leads to a failure of the whole battery pack, results in a pack failure rate of $\lambda_{pack_{rear}} = 5177 \cdot 5.8 \cdot 10^{-9} = 3.0 \cdot 10^{-5}$ and $\lambda_{pack_{main}} = 2505 \cdot 5.8 \cdot 10^{-9} = 1.45 \cdot 10^{-5}$ for the battery packs used within the above presented multirotor case study. Based on the experience of the lithium NCA battery cells used within the Boeing 787, it could be deducted that the pack experienced 3 failures per 250,000 h which corresponds to a failure rate of $1.2 \cdot 10^{-5}$ [50]. According to the analysis of Weigl et al. [51], the lithium-ion batteries of electric vehicles have a Mean Time Between Failures (MTBF) of 19, 106 with a standard deviation of 5918 which corresponds to failure rates between $4.0 \cdot 10^{-5}$ and $7.6 \cdot 10^{-5}$.

Consequently, the assumed battery failure rate within this paper of $9.3 \cdot 10^{-5}$ is still more than 20 % worse than maximum failure rate from the literature research, which is expected to cover the adverse operating conditions with high discharge rates and unfavorable charge–discharge cycles of the multirotor use case. To counteract these effects, short maintenance interval and highest manufacturing as well as processing quality are advised to lower the failure rates and prolong the battery life. Lower future battery failure rates might have the effect that the propulsion system reliability will be increased or even less battery packs are required.

Motor controller failure rates

In the following, the applied failure rate of $4.75 \cdot 10^{-5}$ for the motor controller shall be put into context.

The most failure prone parts within a motor controller are the switching devices which are usually semiconductor IGBTs [54]. As they undergo high electrical and thermal stresses, the dominant failure effect is solder fatigue failure followed by short-circuit or gate open circuit failures [54]. With increasing temperatures of the power electronic, the Mean Time To Failure (MTTF) reduces dramatically as shown within Sathik et al. [54] and Yang et al. [55]. Additionally, increasing the system voltage also increases the risk of motor voltage spikes, breakdown of winding insulation, EMI difficulties which negatively impact the failure rate of power electronic [14, 56]. For IGBT modules used within aircraft that are operating at typical cruising altitudes, the impact of cosmic ray failures compared to wear-out failures needs to be considered predominantly [56]. According to Harikumaran et al. [56], silicon-based IGBT modules used in aviation can provide sufficient reliability up to 540 V system voltages if they are composed of an internal redundancy of two layers. At system voltages above 810 V, reliability is drastically reduced [56].

The literature review of failure rates showed that according to Yang et al. [55], the failure rate of generally used power electronic converters, more specifically IGBT modules, continuously dropped from 20 FIT in the year 2000 to now only few FIT, which equals to a failure rate of $< 2 \cdot 10^{-8}$. A method to calculate the lifetime of power controllers specifically used in aviation which takes into account device degradation and failure effects is presented in Sathik et al. [54]. For a 150 V power controller, a Mean Time To Failure (MTTF) of $6.3 \cdot 10^4$ h as well as a useful lifetime of $3.4 \cdot 10^4$ h was calculated, which converts into failure rates of $1.6 \cdot 10^{-5}$ up to $2.9 \cdot 10^{-5}$. The chosen failure rate for the motor controller of $9.3 \cdot 10^{-5}$ is based on the failure rate used within Darmstadt et al. [13], who refer to aircraft maintenance data in combination with a 270 V system voltage and incorporate an environmental factor of 10 to account for additional adverse operating conditions.

Compared to the literature review, the failure rate of $9.3 \cdot 10^{-5}$ is about 3 times more conservative than the worst identified failure rate by Sathik et al. [54]. As the intended motor controller is assumed to operate at 600 V, the failure rate must be suspected to be higher than calculated by Sathik et al. [54]. As 540 V systems, that are build correspondingly, can still provide sufficient reliability according to Harikumaran et al. [56], it is suspected that the conservative approach with a margin of factor 3 covers those adverse operating conditions and therefore seems acceptable for the preliminary design. However, future analysis should be conducted concerning this topic.

Remaining propulsion system component failure rates

The failure rates of the electric motor, gearbox, flight control computer, power relay and disconnect clutch are also chosen conservatively and are based on actual failure rates collected within the NPRD from components used within the aviation context [35]. The failure rates for the electric

motor and the gearbox are additionally devaluated by an environmental factor of 10 to account for adverse operating conditions during the eVTOL operation. Lower than assumed failure rates will increase the overall propulsion reliability and potentially decrease the system weight due to less required redundancy.

Appendix C: Supplementary Propulsion System Design Information

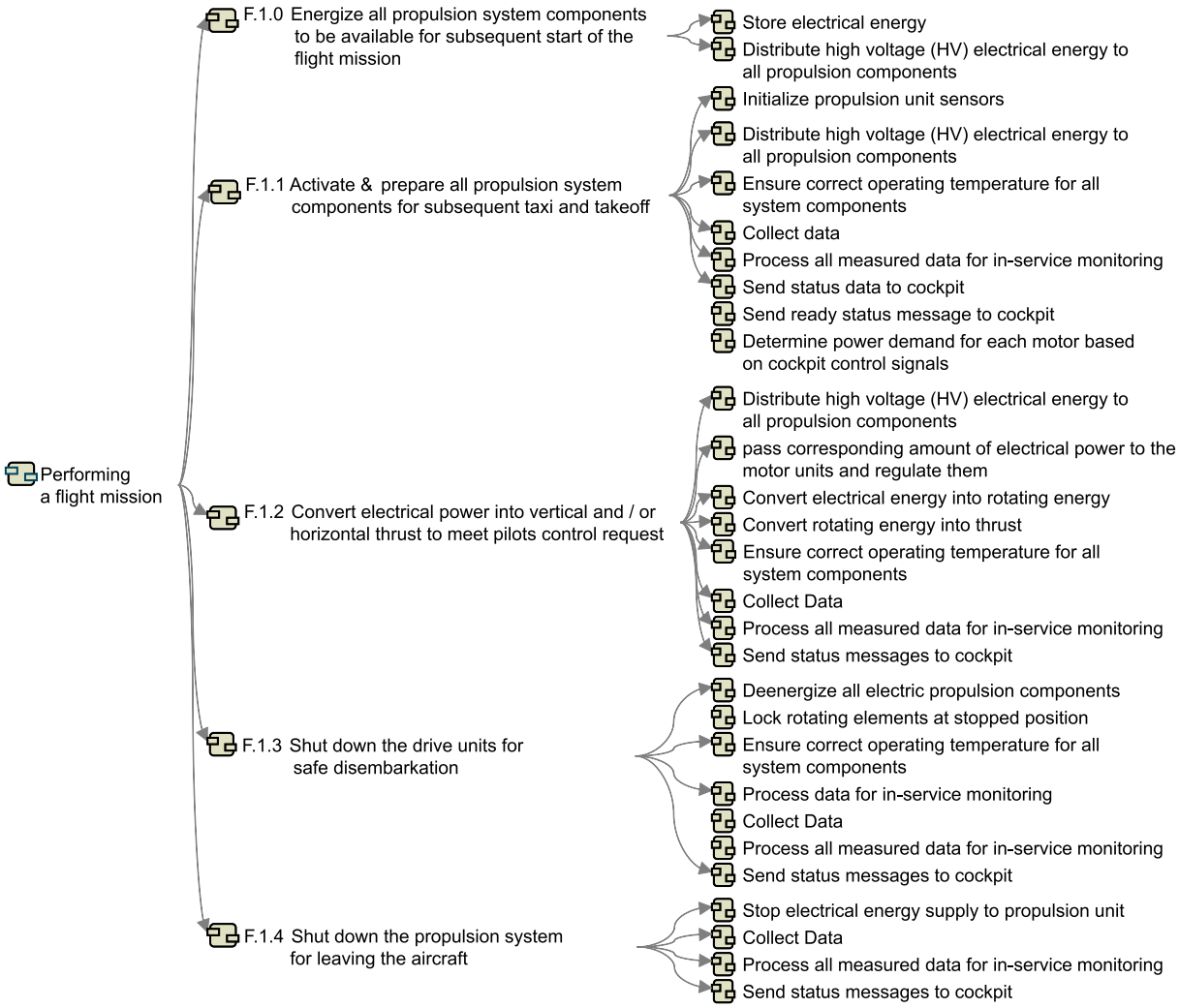

Fig. 24 Propulsion system function analysis

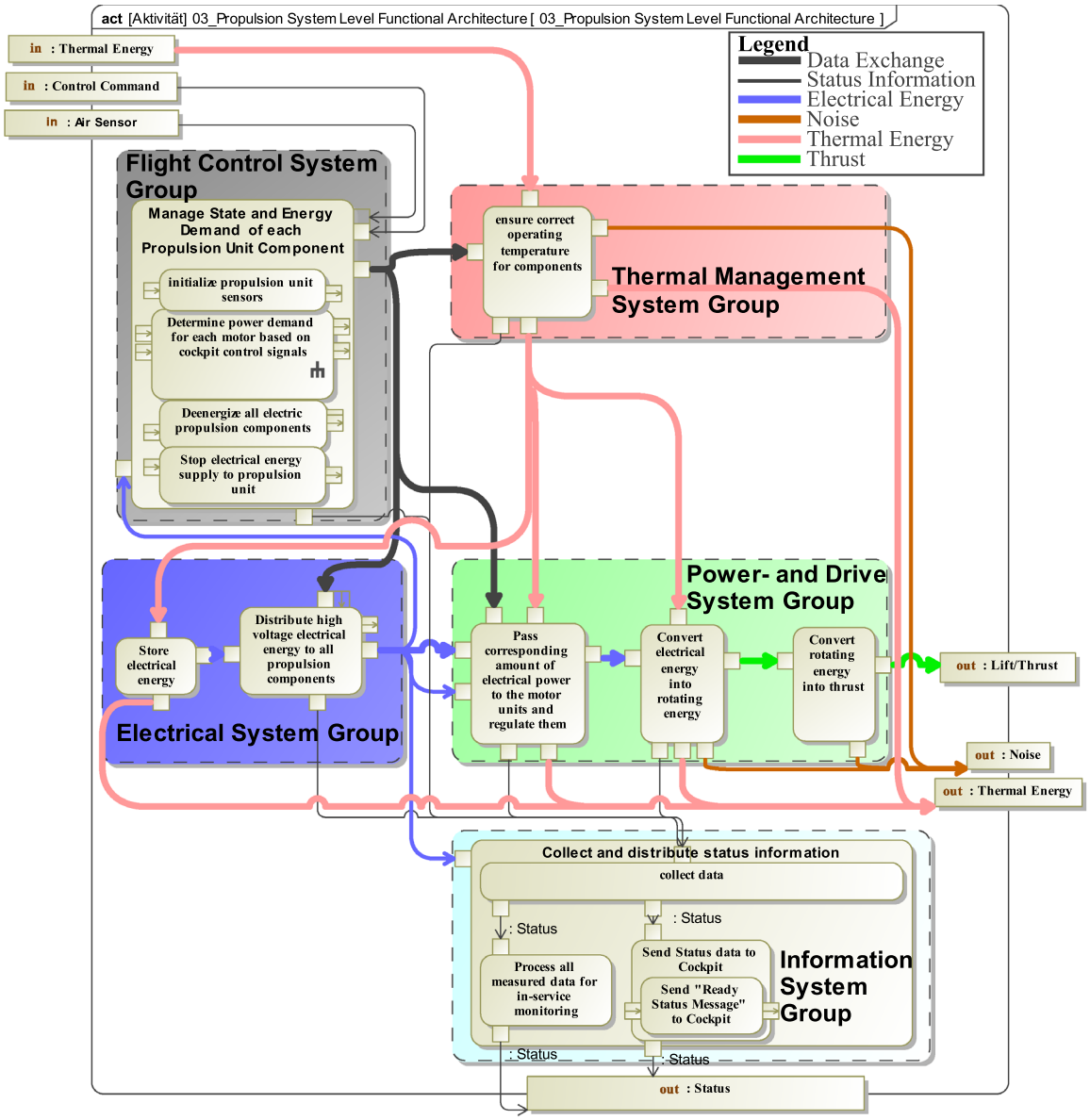

Fig. 25 Functional block diagram of the propulsion system

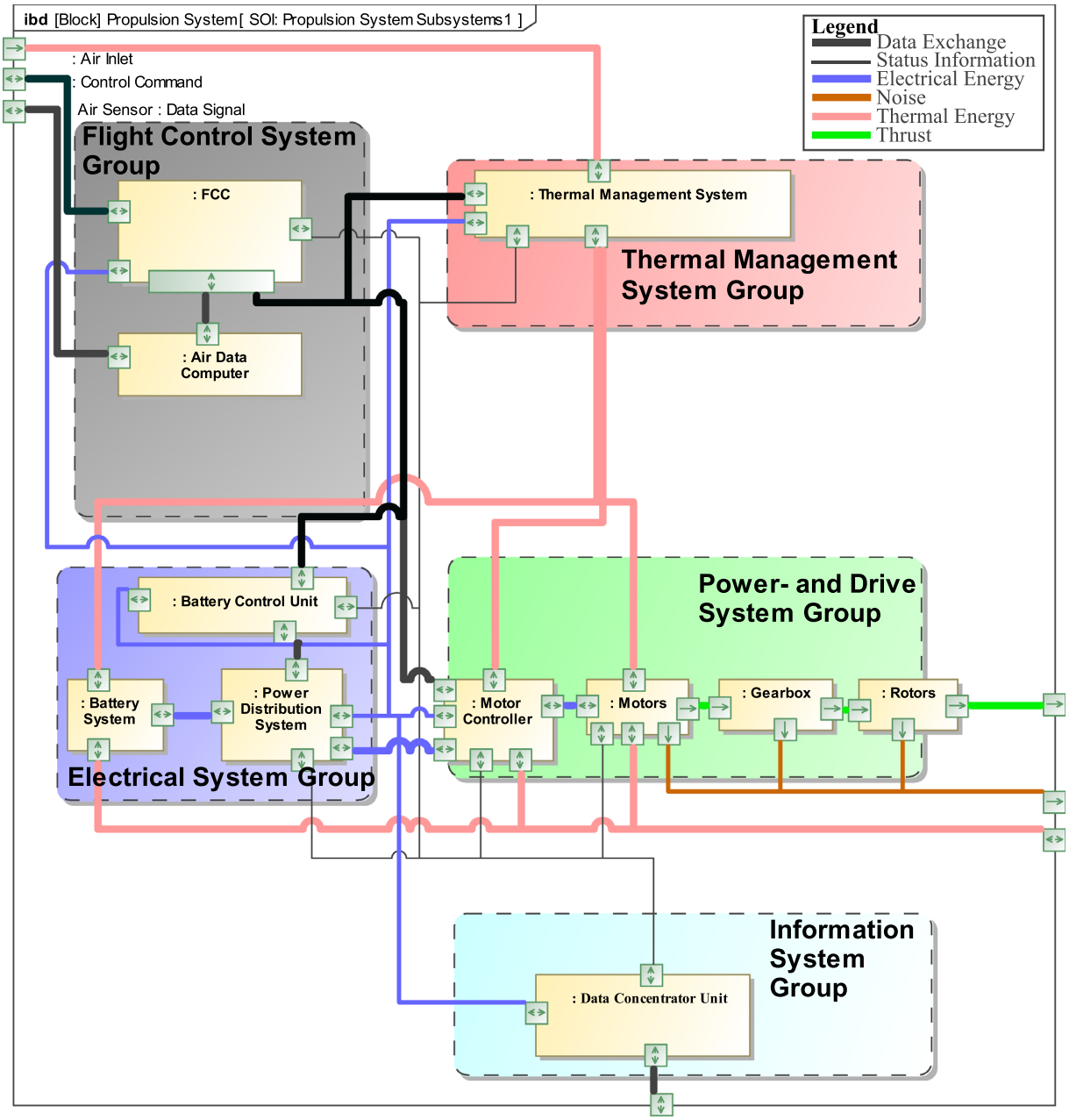

Fig. 26 Logical Architecture of the Propulsion System

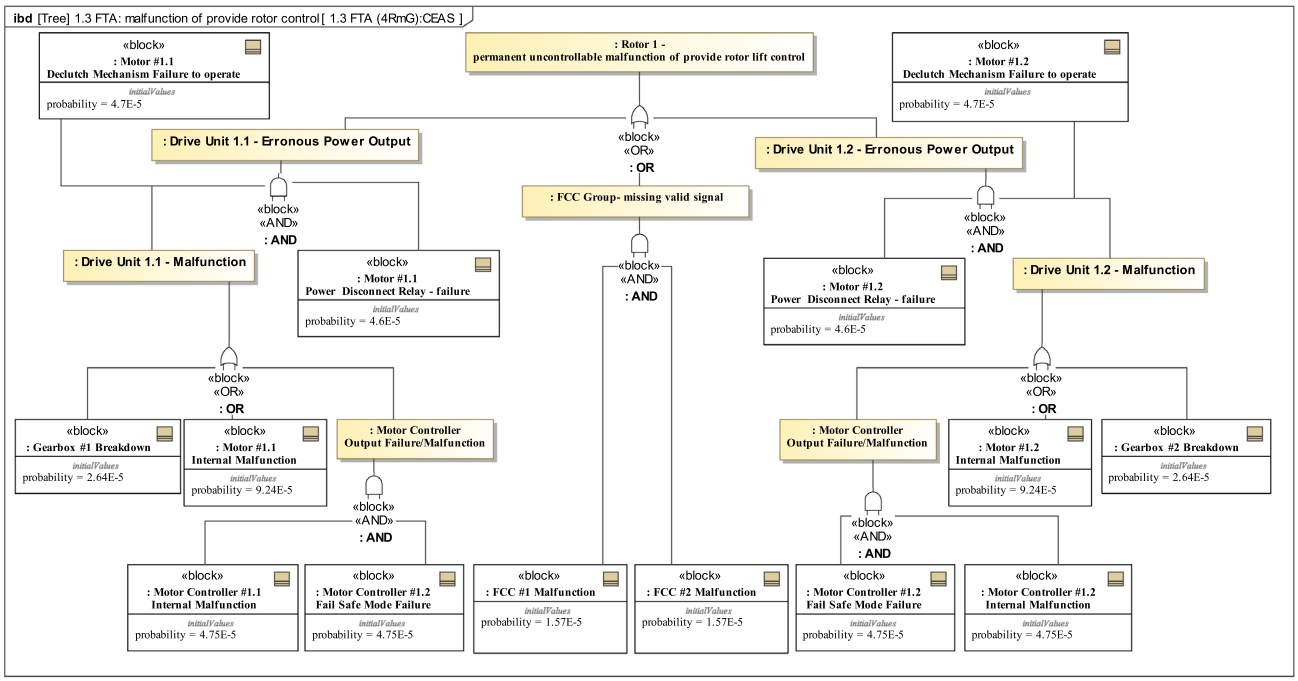

Fig. 27 System FTA for the permanent incorrect operation of one rotor lift

Acknowledgements The paper presents results from the internal DLR project HorizonUAM.

Author Contributions Conceptualization: FJ; methodology: FJ, OB; writing—original draft preparation: FJ, OB, SML, AHB, JR, LB; writing—review and editing: FJ; supervision: OB; project administration, OB; all authors have read and agreed to the published version of the manuscript.

Funding Open Access funding enabled and organized by Projekt DEAL.

Data availability All required data supporting the findings of this study are included within this paper. Further data can be found in previous publications and are avialable from the corresponding author upon reasonable request.

Declarations

Conflict of interest The authors have no conflict of interest to declare that are relevant to the content of this article.

References

1. Ritchie, H., Roser, M.: Urbanization. OurWolrdInData.org (2018). https://ourworldindata.org/grapher/urban-and-rural-population-2050 Accessed 2023-01-15
2. Pishue, B.: INRIX 2022 Global Traffic Scorecard. INRIX (2023)
3. Goyal, R., Reiche, C., Fernando, C., Serrao, J., Kimmel, S., Cohen, A., Shaheen, S.: Urban air mobility (UAM) market study (No. HQ-E-DAA-TN65181) (2018)
4. Rothfeld, R., Fu, M., Balać, M., Antoniou, C.: Potential urban air mobility travel time savings: an exploratory analysis of Munich, Paris, and San Francisco. Sustainability **13**(4), 2217 (2021). https://doi.org/10.3390/su13042217
5. Ritchie, H., Roser, M., Rosado, P.: Energy. Our World In Data (2022). https://ourworldindata.org/transport#co2-emissions-by-mode-of-transport Accessed 2023-01-15
6. André, N., Hajek, M.: Robust environmental life cycle assessment of electric VTOL concepts for urban air mobility. In: AIAA Aviation 2019 Forum, p. 3473 (2019). https://doi.org/10.2514/6.2019-3473
7. EUROCONTROL: EUROCONTROL Data Snapshot. Half of CO2 Emissions come from just 6 % of fights: the long-haul ones. EUROCONTROL (2021). https://www.eurocontrol.int/publication/eurocontrol-data-snapshot-co2-emissions-flight-distance
8. Baumeister, S., Leung, A., Ryley, T.: The emission reduction potentials of first generation electric aircraft (FGEA) in Finland. J. Trans. Geography **85**, 102730 (2020). https://doi.org/10.1016/j.jtrangeo.2020.102730
9. Staack, I., Sobron, A., Krus, P.: The potential of full-electric aircraft for civil transportation: from the Breguet range equation to operational aspects. CEAS Aeronaut. J. **12**(4), 803–819 (2021). https://doi.org/10.1007/s13272-021-00530-w
10. Electric VTOL News: eVTOL Aircraft Directory. The Vertical Flight Society. https://evtol.news/aircraft Accessed 2023-02-28

11. Cohen, A.P., Shaheen, S.A., Farrar, E.M.: Urban air mobility: history, ecosystem, market potential, and challenges. IEEE Trans. Intell. Trans. Syst. **22**(9), 6074–6087 (2021). https://doi.org/10.1109/TITS.2021.3082767
12. EASA: Special Condition for small-category VTOL aircraft. EASA SC-VTOL-01 (1) (2019)
13. Darmstadt, P.R., Catanese, R., Beiderman, A., Dones, F., Chen, E., Mistry, M.P., Babie, B., Beckman, M., Preator, R.: Hazards Analysis and Failure Modes and Effects Criticality Analysis (FMECA) of Four Concept Vehicle Propulsion Systems (No. NASA/CR-2019-220217) (2019)
14. Darmstadt, P.R., Pathak, S., Chen, E., Mistry, M.P., Arkebauer, A., Beiderman, A., Dillard, C., Zierten, D., Beckman, M., Monroe, A.: Reliability and Safety Assessment of Urban Air Mobility Concept Vehicles (No. GTRI Document No. D9015A001R2) (2021)
15. Liscouët, J., Pollet, F., Jézégou, J., Budinger, M., Delbecq, S., Moschetta, J.-M.: A methodology to integrate reliability into the conceptual design of safety-critical multirotor unmanned aerial vehicles. Aerospace Science and Technology (127), 107681 (2022) https://doi.org/10.1016/j.ast.2022.107681.
16. Bertram, O., Jäger, F., Voth, V., Rosenberg, J.: UAM Vehicle Design with Emphasis on Electric Powertrain Architectures. AIAA SciTech 2022 Forum, 1995 (2022) https://doi.org/10.2514/6.2022-1995
17. SAE International: Guidelines and Methods for Conducting the Safety Assessment Process on Civil Airborne Systems and Equipment (ARP4761) (1996) https://doi.org/10.4271/ARP4761
18. SAE International: Guidelines for Development of Civil Aircraft and Systems (ARP4754A) (2010) https://doi.org/10.4271/ARP4754A
19. EASA: Electric / Hybrid Propulsion System. SC E-19 (Issue 1) (2021)
20. EASA: Certification Specifications for Propellers. CS-P (Issue 1) (2003)
21. Ratei, P.: Conceptual Aircraft Design and Comparison of different eVTOL Aircraft for Urban Air Mobility. Hamburg University of Applied Sciences (HAW Hamburg) (2021)
22. Bertram et al.: Impact of different Powertrain Architectures on UAM Vehicle Concepts. In: Deutscher Luft- und Raumfahrtkongress, Virtual (2021)
23. Pavel, M.D.: Understanding the control characteristics of electric vertical take-off and landing (eVTOL) aircraft for urban air mobility. Aerospace Sci. Technol. **125**, 107143 (2021). https://doi.org/10.1016/j.ast.2021.107143
24. Bahr, M., McKay, M., Niemiec, R., Gandhi, F.: Handling qualities of fixed-pitch, variable-speed multicopters for urban air mobility. Aeronaut. J. **126**(1300), 952–972 (2022). https://doi.org/10.1017/aer.2021.114
25. Niemiec, R., Gandhi, F., Lopez, M., Tischler, M.: System Identification and Handling Qualities Predictions of an eVTOL Urban Air Mobility Aircraft Using Modern Flight Control Methods. In: Vertical Flight Society 76th Annual Forum, Virtual (2020)
26. Atci, K., Jones, M., Jusko, T.: Assessment of the Handling Qualities of Multirotor Configurations using Real Time Simulation. In: Deutscher Luft- und Raumfahrtkongress 2021 (2021). https://doi.org/10.25967/550236
27. Atci, K., Weiand, P., Guner, F.: Understanding the fixed pitch RPM-controlled rotor modeling for the conceptual design of UAM vehicles. CEAS Aeronaut. J. **15**, 409–422 (2024). https://doi.org/10.1007/s13272-023-00703-9
28. Atci, K., Jusko, T., Strbac, A., Guner, F.: Impact of Differential Torsional Rotor Cant on the Flight Characteristics of a Passenger-Grade Quadrotor. CEAS Aeronautical Journal, 1–12 (2024) https://doi.org/10.1007/s13272-023-00705-7
29. Gong, X., Fenech, B., Blackmore, C., Chen, Y., Rodgers, G., Gulliver, J., Hansell, A.L.: Association between noise annoyance and mental health outcomes: a systematic review and meta-analysis. Int. J. Environ. Res. Publ. Health **19**(5), 2696 (2022). https://doi.org/10.3390/ijerph19052696
30. Brown, A., Harris, W.L.: A Vehicle Design and Optimization Model for On-Demand Aviation. In: 2018 AIAA/ASCE/AHS/ASC Structures, Structural Dynamics, and Materials Conference, p. 0105 (2018). https://doi.org/10.2514/6.2018-0105
31. Smith, B., Gandhi, F., Niemiec, R.: A comparison of Multicopter Noise Characteristics with Increasing Number of Rotors. In: 76th Annual Forum of the Vertical Flight Society, Virtual (2020)
32. Smith, B., Healy, R., Gandhi, F., Lyrintzis, A.: eVTOL Rotor Noise in Ground Effect. In: Vertical Flight Society's 77th Annual Forum & Technology Display (2021)
33. Herrmann, F., Rothfuss, F.: Introduction to Hybrid electric vehicles, battery electric vehicles, and off-road electric vehicles. In: Scrosati, B., Garche, J., Tillmetz, W. (eds.) Advances in Battery Technologies for Electric Vehicles. Woodhead Publishing, pp. 3–16 (2015). https://doi.org/10.1016/B978-1-78242-377-5.00001-7
34. Schäfer, M., Berres, A., Bertram, O.: Integrated model-based design and functional hazard assessment with SysML on the example of a shock control bump system. CEAS Aeronaut. J. **14**(1), 187–200 (2023). https://doi.org/10.1007/s13272-022-00631-0
35. Quanterion Solutions Incorporated: Nonelectronic Parts Reliability Data, (2016)
36. Dubrova, E.: Fault-Tolerant Design. Springer New York, NY (2013) https://doi.org/10.1007/978-1-4614-2113-9
37. Asmer, L., Pak, H., Prakasha, P.S., Schuchardt, B.I., Weiand, P., Meller, F., Torens, C., Becker, D., Zhu, C., Schweiger, K.: Urban air mobility use cases, missions and technology scenarios for the HorizonUAM project. In: AIAA Aviation 2021 Forum, p. 3198 (2021). https://doi.org/10.2514/6.2021-3198
38. OMG: Risk analysis and assessment modeling language (RAAML). Object Management Group, OMG (2020). https://www.omg.org/spec/RAAML Accessed 2023-03-06
39. Bevirt, J., Stoll, A., Geest, M., MacAfee, S., Ryan, J.: Electric Power System Architecture and Fault Tolerant VTOL Aircraft Using Same. US Patent 11,827,347 B2, November 28, 2023. https://patentimages.storage.googleapis.com/4a/b9/c7/346c3c8a6ee568/US11827347.pdf
40. EMRAX d.o.o.: EMRAX 348 Technical Data Table. EMRAX d.o.o (05.03.2020). https://emrax.com/wp-content/uploads/2020/03/emrax_348_technical_data_table_graphs_5.4.pdf Accessed 2021-06-25
41. EMRAX d.o.o.: EMRAX 228 Technical Data Table. EMRAX d.o.o (05.03.2020). https://emrax.com/wp-content/uploads/2022/11/EMRAX_228_datasheet_A00.pdf Accessed 2023-08-29
42. Nandi, S., Toliyat, H.A., Li, X.: Condition monitoring and fault diagnosis of electrical motors-A review. IEEE Trans. Energy Conversion **20**(4), 719–729 (2005)
43. Energy Company of Panasonic Group: Introduction of NCR18650PF. Panasonic (2013). https://www.akkuparts24.de/mediafiles/Datenblaetter/Panasonic/Panasonic%20NCR-18650PF.pdf Accessed 2023-05-31
44. Schmalstieg, J., Käbitz, S., Ecker, M., Sauer, D.U.: A holistic aging model for Li(NiMnCo)O2 based 18650 lithium-ion batteries. J. Power Sources **257**, 325–334 (2014). https://doi.org/10.1016/j.jpowsour.2014.02.012
45. Shiotani, S., Naka, T., Morishima, M., Yonemura, M., Kamiyama, T., Ishikawa, Y., Ukyo, Y., Uchimoto, Y., Ogumi, Z.:

Degradation analysis of 18650-type lithium-ion cells by operando neutron diffraction. J. Power Sources **325**, 404–409 (2016). https://doi.org/10.1016/j.jpowsour.2016.06.026
46. Bills, A., Sripad, S., Fredericks, L., Guttenberg, M., Charles, D., Frank, E., Viswanathan, V.: A battery dataset for electric vertical takeoff and landing aircraft. Sci. Data **10**(1), 344 (2023). https://doi.org/10.1038/s41597-023-02180-5]
47. Duh, Y.S., Sun, Y., Lin, X., Zheng, J., Wang, M., Wang, Y., Lin, X., Jiang, X., Zheng, Z., Zheng, S.: Characterization on thermal runaway of commercial 18650 lithium-ion batteries used in electric vehicles: A review. J. Energy Storage **41**, 102888 (2021). https://doi.org/10.1016/j.est.2021.102888
48. Vedachalam, N., Vandavasi, B.N.J.: Role of Lithium-Ion batteries in increasing the operational safety of offshore service vessels. Marine Technol. Soc. J. **55**(6), 174–185 (2021). https://doi.org/10.4031/MTSJ.55.6.13
49. Meteostat: Wetterrückblick und Klimadaten. Meteostat. https://meteostat.net/de/ Accessed 2023-06-13
50. Kolly, J.M., Panagiotou, J., Czech, B.A.: The investigation of a Lithium-Ion Battery Fire Onboard a Boeing 787 by the US National Transportation Safety Board. Safety Research Corporation of America: Dothan, AL, USA, 1–18 (2013)
51. Weigl, D., Inman, D., Hettinger, D., Ravi, V., Peterson, S.: Battery Energy Storage Scenario Analyses Using the Lithium-Ion Battery Resource Assessment (LIBRA) Model. National Renewable Energy Laboratory (NREL), Golden, CO (United States) (No. NREL/TP-6A20-81875) (2022) https://doi.org/10.2172/1899991
52. Sivert, A., Betin, F., Vacossin, B., Lequeu, T., Dondon, P.: Lithium battery: diagnostics and lifespan. Application to the range estimation of an electric vehicle. WSEAS Transactions on Environment and Development **13**, 10–18 (2017)
53. Ohneseit, S., Finster, P., Floras, C., Lubenau, N., Uhlmann, N., Seifert, H.J., Ziebert, C.: Thermal and mechanical safety assessment of type 21700 lithium-ion batteries with NMC, NCA and LFP cathodes-investigation of cell abuse by means of accelerating rate calorimetry (ARC). Batteries **9**(5), 237 (2023). https://doi.org/10.3390/batteries9050237
54. Sathik, M.H.M., Prasanth, S., Sasongko, F., Pou, J.: Lifetime estimation of off-the-shelf aerospace power converters. IEEE Aerospace Electron Syst Mag **33**(12), 26–38 (2018). https://doi.org/10.1109/MAES.2018.180030
55. Yang, S., Xiang, D., Bryant, A., Mawby, P., Ran, L., Tavner, P.: Condition monitoring for device reliability in power electronic converters: a review. IEEE Trans Power Electron **25**(11), 2734–2752 (2010). https://doi.org/10.1109/TPEL.2010.2049377
56. Harikumaran, J., Buticchi, G., Migliazza, G., Madonna, V., Giangrande, P., Costabeber, A., Wheeler, P., Galea, M.: Failure modes and reliability oriented system design for aerospace power electronic converters. IEEE Open J. Ind. Electron. Soc. **2**, 53–64 (2021). https://doi.org/10.1109/OJIES.2020.3047201